Symplasmic pathway in phloem loading and unloading in source and sink leaves of *Zea mays* L as evidenced under normal and elevated CO_2 conditions.

Thesis submitted in fulfilment of the
requirements of the degree of

Master of Science
of
Rhodes University

by

NOLUYOLO NOGEMANE

February 2003

ABSTRACT

Zea mays plants kept at ambient (ca 375ppm) and elevated CO_2 (ca 650 to 700ppm) were used to examine the possibility of a symplasmic loading, unloading and transport pathway in dark-adapted and illuminated (200μmolm^{-2}sec^{-1}) sink and source leaves. 5,6-carboxyfluorescein diacetate was introduced into the mesophyll cells and symplasmic transfer observed 3h after application. In sink and source leaves exposed to ambient CO_2 and illuminated at 200 molm^{-2}sec^{-1}, the fluorescence front was observed approximately 3cm from the point of application, while in dark-adapted plants, the fluorescence front was observed approximately 1cm from the point of application. Under elevated CO_2 conditions the fluorescence front in illuminated plants appeared to transport faster moving approximately 5cm from the point of application, and in dark-adapted plants, only 3cm from the point of application. Based on the increase in 5,6-CF accumulation under elevated CO_2 conditions, the present study suggests that there was an increase in capacity for assimilate loading and transport under elevated CO_2 conditions. In source leaves, 5,6-CFDA was taken up into the mesophyll cells, loaded symplasmically and transported basipetally. In sink leaves 5,6-CFDA was taken up from basal mesophyll and after symplasmic loading, was transported acropetally where it was offloaded into the younger immature sink region.

Transport in the sieve tubes was confirmed by using aniline blue, which was applied 3h after 5,6-CF transport. Aniline blue coupled with 5,6-CF transport studies showed that the sieve tubes of both cross and longitudinal veins are involved in symplasmic unloading, loading and transport processes in sink and source leaves. Apoplasmic uptake of 5,6-CFDA by cut leaves showed that after apoplasmic transport via the transpiration stream, 5,6-CFDA was offloaded to the xylem parenchyma where it was metabolically cleaved, releasing fluorescent 5,6-CF into the xylem parenchyma.

Transverse sections cut after 3h of uptake were observed after 120 and 180 min suggesting that a retrieval of solutes occurs from the xylem to the xylem parenchyma, bundle sheath, phloem parenchyma and to the thin-walled sieve tubes. It was not possible to determine if the thick-walled sieve tubes were involved or if they took up 5,6-CF.

Given the available data on loading and offloading of assimilates in sink and source leaves respectively, this study demonstrated that a slow symplasmic pathway exists from the mesophyll to the phloem, and that offloading from the phloem in sink leaves can occur via a symplasmic route.

TABLE OF CONTENT

ABSTRACT ... (ii)

ACKNOWLEDGEMENTS ... (v)

LIST OF FIGURES ... (vi)

CHAPTER 1: INTRODUCTION ... **1**

1.1 INTRODUCTION TO PHLOEM LOADING ... 1
1.2 STRUCTURAL CONSIDERATION OF THE PHLOEM LOADING PATHWAY ... 1
1.3 PLASMODESMATA IN THE PHLOEM LOADING PATHWAY ... 5
1.4 SYMPLASMIC LOADING VERSUS APOPLASMIC LOADING ... 12
1.5 THE USE OF FLUORESCENT TRACERS IN PHLOEM LOADING ... 15
1.6 INCREASES IN ATMOSPHERIC CARBON DIOXIDE (CO2) RELATED TO PHLOEM LOADING ... 18
1.7 OBJECTIVES ... 19

CHAPTER 2: MATERIALS AND METHODS ... **21**

2.1 PLANT MATERIAL ... 21
2.2 SAMPLING PROCEDURE ... 22
2.3 LIGHT MICROSCOPY ... 22
2.4 FLUORESCENCE MICROSCOPY ... 23
  2.4.1 Aniline blue fluorescence microscopy ... 23
  2.4.2 Leaf tissue preparation for 5,6 Carboxyfluorescein (5,6-CFDA) application ... 23
  2.4.3 Aniline blue and 5,6-CFDA fluorescence microscopy ... 25
  2.4.4 Preparation of Texas Red ... 25
  2.4.5 Uptake of 5,6-CFDA and Texas Red via the transpiration stream ... 26
2.5 DIGITAL IMAGING ... 27

CHAPTER 3: RESULTS ... **28**

3.1GENERAL ANATOMY OF THE MAIZE LEAF ... 28
3.2 TRANSPORT STUDIES ... 32
  3.2.1 Visualization of the aniline blue-stained callose deposition ... 32
  3.2.2 Visualization of the fluorochrome (5,6-CF) transport within sink leaves ... 37
  3.2.3 Visualization of the fluorochrome within source leaves ... 46
  3.2.4 Visualization of 5.6-CF transport in the cross vein and lateral transfer in sink and source leaves ... 55
  3.2.5 Visualization of 5,6-CF within the sieve tubes in sink and source leaves ... 59
  3.2.6 Apoplasmic retrieval from the xylem to the phloem ... 64

CHAPTER 4: DISCUSSION ... **69**

4.1 ANATOMY OF THE LEAF ... 69
4.2 HIGH CO$_2$ EFFECTS ON TRANSPORT ... 69
4.3 IMPLICATION OF PLASMODESMATA IN SYMPLASMIC LOADING AS VISUALIZED VIA ANILINE BLUE FLUORESCENCE ... 72
4.4 DOES ZEA MAYS LEAF BLADE PHLOEM LOAD SYPLASMICALLY? ... 73
4.5 THE ROLE OF THE THIN- AND THICK-WALLED SIEVE TUBES ... 78
4.6 APOPLASTIC RETRIEVAL FROM THE XYLEM TO THE PHLOEM ... 81
4.7 PHLOEM AND XYLEM TRANSPORT AS VISUALIZED VIA 5,6-CF AND TEXAS RED ... 82

CHAPTER 5: CONCLUSIONS ... **83**

REFERENCES ... **86**

APPENDIX A **97**
MACRONUTRIENT 97
MICRONUTRIENT 97
APPENDIX B **97**

List of Figures **Page**

Figure 3.1	Detailed anatomical structure at transverse and paradermal sections	28
Figure 3.2	Localization of callose in the leaf blade as shown at paradermal sections	33
Figure 3.3	Visualization of 5,6-CF at paradermal section in sink leaves exposed to ambient CO_2	37
Figure 3.4	Visualization of 5,6-CF at paradermal sections in sink leaves exposed to elevated CO_2	41
Figure 3.5	Visualization of 5,6-CF at paradermal sections in source leaves exposed to ambient CO_2	47
Figure 3.6	Visualization of 5,6-CF at paradermal sections in source leaves exposed to elevated CO_2	51
Figure 3.7	Visualization of 5,6-CF at paradermal sections in sink and source leaves exposed to ambient CO_2	55
Figure 3.8	Visualization of 5,6-CF and aniline blue at paradermal sections in sink and source leaves exposed to ambient CO_2	59
Figure 3.9	Visualization of 5,6-CF and 3-kD Texas red at transverse sections in sink leaves.	65

Acknowledgements

Firstly I must acknowledge and thank my Supervisor, Prof Botha for giving me the opportunity of researching towards an MSc degree under his excellent supervision in the ecophysiology laboratory.

My thanks are also due to those who helped with the final preparation of this thesis, Mrs. Abrahams in the Graphic unit.

My fellow students of the Botany department are thanked for their support, especially the Ecophysiology postgraduate group. I also would like to pass my special thanks to all my friends who were always there to give moral support.

I am most grateful to my parents for their constant encouragement and interests in my academic progress and for offering financial support whenever I was in need. Mom and Dad, without you I would not have been where I am today.

Lastly, financial support from the National Research foundation (NRF, Pretoria, SA) that awarded an MSc bursary is acknowledged.

CHAPTER 1: INTRODUCTION

1.1 Introduction to phloem loading

Translocation of assimilates from the photosynthesizing cells in the leaves to the growing tissues; seeds and storage organs are the basis of plant performance and agricultural yield (Komor 2000). Studies in plant metabolism, cellular and anatomical structures and new methods in cell biology led to rapid progress in phloem transport and physiology. Geiger (1975) defined phloem loading as the process by which the major translocated substances are selectively and possibly actively delivered from the mesophyll cells to the sieve tubes in the source region prior to translocation. It is the initial step in the transport of photoassimilates (products of photosynthesis) from source regions of the plant to the sinks. This process is essential not only for the transport of sugars but also for the translocation of all other compounds present in the phloem, including amino acids and the xenobiotics

1.2 Structural consideration of the phloem loading pathway

Knowledge of the phloem loading pathway is essential to our understanding of how plants transport photosynthates to sinks where these assimilates are used. In common with the leaves of other grasses, those of *Zea mays* have numerous parallel or longitudinal vascular bundles. A detailed study by Russell and Evert (1985) showed that the longitudinal bundles of the leaf blade fall roughly into 3 groups according to size and structure (large, intermediate and small bundles), which alternate fairly regularly with one another and are interconnected by small transverse veins. These different groups of bundles serve different functions within the leaves of C_4 and C_3 species studied to date (Lush, 1976; Altus & Canny, 1982; Evert, 1986; Evert & Mierzwa, 1989; Fritz *et al.* 1989; Evert *et al.* 1996; Botha & Cross, 1997). Larger veins have been reported to be primarily involved with long distance transport, while intermediate and small veins were active in the collection of photosynthates, short distant movement or in the accumulation and storage of photosynthetic products.

Studies undertaken by several authors have shown that the small and intermediate bundles of the *Zea mays* leaf blade contain two kinds of sieve tubes, that is, thin- and thick-walled sieve tubes (Evert *et al.* 1978; Evert, 1980; Evert & Russin, 1993; Evert *et al.* 1996 and papers cited) These are classified as early-formed and late-formed metaphloem respectively. When only two sieve tubes are present, they always differ from one another, in other words, one will be thick-walled and the other will be thin-walled. The early-formed metaphloem fits the classical description of phloem, in that it is associated with parenchymatic elements generally regarded as companion cells. These are called thin-walled sieve tubes because their walls are thin compared to the late-formed sieve tubes. The late-formed metaphloem sieve tube lack companion cells (Walsh, 1974; Evert *et al.* 1978) and differentiate next to the metaxylem vessels. Less often they are separated from the xylem by intervening vascular parenchyma. More recently it has been reported that the late-formed sieve tubes in maize are also characterized by the presence of tubular extensions of plasmalemma (Evert *et al.* 1977), hence the term thick-walled sieve tubes will be used.

The lateral or transverse veins contain usually only one sieve tube, and this is usually the thin-walled sieve tube (Evert *et al.* 1978). This sieve tube is associated with a companion cell, a tracheary element and if present one or two vascular parenchyma cells. The sieve tubes of the lateral veins connect directly to the thin-walled sieve tubes of the longitudinal veins. Whilst transport between veins must occur via the thin-walled sieve tube, longitudinal transport within the phloem in three vein size classes could occur via either the thin- and/or the thick-walled sieve tubes, provided that there are sufficient plasmodesmata at that site.

The presence of two types of sieve tubes in grass leaves has led to a great deal of speculation about their function. Based on the close spatial association of the thick-walled sieve tubes with the vessel, and on their possession of the plasmalemma tubules, Evert *et al.* (1978) suggested that the thick-walled sieve tubes may play a role in the retrieval of solutes entering the leaf apoplast from the transpiration stream. In microautoradiographic studies carried out by Fritz *et al.* (1983) it was observed that the thick-walled sieve tubes receive photosynthates transferred from the vascular parenchyma during solute retrieval. However these authors suggested that thick-walled sieve tubes in maize are not involved in long distance transport, but could quickly shunt their contents laterally to thin-walled sieve tubes of larger bundles via the sieve tube of transverse veins.

Both the thin- and the thick- walled sieve tube of longitudinal bundles are connected to the sieve tube of the transverse vein.

Export of assimilates from the blade takes place via the thin-walled sieve tube of large and that of intermediate bundles extending basipetally into the leaf sheath and stem (Evert, 1986). These thin-walled sieve tubes are associated with companion cells, referred to as 'traffic control' centres of the phloem (Oparka and Turgeon, 1999). Esau (1977) regarded these cells as intermediary cells specialized for the uptake of sugar and its delivery into these sieve tubes (see also Giaquinta, 1980; Warmbrodt & Van Der Woude, 1990; van Bel & Knoblauch, 2000). Lack of companion cells associated with the thick-walled sieve tube suggests either that this sieve tube is non-functional or that the role of companion cells has been taken over by parenchymatous cells associated with them. Studies by Fritz *et al.* (1983) showed that thin-walled sieve tubes are capable of accumulating sucrose and photosynthates from the apoplast without companion cells acting as intermediary cells.

Matsiliza and Botha (2002) studied the feeding preference of the Aphid, *Stobion yakini* on leaf blades of barley, which demonstrated that the aphids fed preferentially on thin-walled sieve tubes. Matsiliza and Botha (2002) argued this to be perhaps caused by greater quantities of assimilates transported in the thin-walled than in the thick-walled sieve tubes, suggesting that the thin-walled sieve tubes may be more functional and play an important role in phloem loading and transport.

Investigation on the small and intermediate bundles of *Zea mays* leaf by Evert *et al.* (1978) showed that the thick-walled sieve tubes have numerous pore plasmodesmatal connections with the vascular parenchyma cells whilst the corresponding thin-walled sieve tubes have numerous pore plasmodesmatal connections with their companion cells. Plasmodesmatal connections between the thin-walled sieve tube companion cell complex (CWST/CC) and other cell types of the leaf, including vascular parenchyma and thick-walled sieve tube, were reported to be rare. Evert *et al.* (1978) concluded that, the thin-walled sieve tube companion cell complex is virtually isolated symplasmically from the rest of the leaf.

1.3 Plasmodesmata in the phloem loading pathway

Plasmodesmata are narrow threads or extensions of cytoplasm that pass through adjacent cell walls and affords continuity and connections between plant cells. Plasmodesmatal connectivity in plants is thought to reflect the pathway of loading and has been invoked to support the claims concerning the mechanism of phloem loading. But the structure, frequency and distribution, and plasmodesmatal function must be considered between all cell types in order to explain a potential phloem loading pathway (Warmbrodt & Van Der Woude, 1990; Beebe & Evert, 1992; Gamalei, 1996; Russin *et al.* 1996; Van Bel & Knoblauch, 2000).

Over the past years, investigators have collected data on the plasmodesmatal frequencies and distribution between the mesophyll and the sieve element-companion cell complex in the minor veins of leaves (Turgeon *et al.* 1975; Gunning, 1976; Evert *et al.* 1978; Gamalei & Pakhomova, 1981; Fischer & Evert, 1982; Russin & Evert, 1985; Evert & Mierzwa, 1986; Fisher, 1986; Botha & Evert, 1988; Botha, 1990; Robinson & Evert, 1991; Evert *et al.* 1996; Botha & Cross, 1997). Originally plasmodesmatal frequencies were listed in tables. On rearrangement of the data into plasmodesmograms it was possible to visualize the existence of several forms of phloem loading (van Bel *et al.* 1988; Botha & van Bel, 1992). Based on plasmodesmograms, two pathways associated with specific modes of phloem loading were postulated: symplasmic and apoplasmic phloem loading pathways. Proponents of an entirely symplasmic pathway visualized the movement of assimilates from the mesophyll cells to the sieve tubes via the plasmodesmata in their common walls (Cataldo, 1974; Madore & Webb, 1981). Those favouring the entirely apoplasmic pathway proposed that sugars formed in the mesophyll cells are moved across the cell wall interfaces in the absence of plasmodesmata at some point in the pathway, that is, transport from the symplast into the apoplast space and then taken up into the sieve tubes (Giaquinta, 1983).

Given the above, one could assume that abundant plasmodesmata at pertinent cell interfaces along the pathways is generally interpreted as favouring symplasmic transport and possible symplastic loading, whereas a paucity of plasmodesmata anywhere along the way maybe regarded as favouring an apoplasmic phase at such sites.

Plasmodesmal frequency decreases along the loading route from mesophyll cell to the sieve element/companion cell complex, and increase along the unloading pathway in the opposite direction to compensate for the increase in surface area to volume ratio (Evert *et al.* 1978; Ding *et al.* 1988; Botha, 1992; Evert *et al.* 1996). This may at least partly account for the low frequency of plasmodesmata between the sieve element-companion cell and the surrounding cells in most species studied to date. It is therefore not possible to argue that the loading pathway has to be apoplasmic, simply because the frequency of plasmodesmata leading into the sieve element-companion cell complex is low. Giaquinta (1989) stated that the number of functioning plasmodesmata, and not the absolute count of plasmodesmata, determines the efficiency of symplasmic transport. And hence the functionality of plasmodesmata has to be considered before symplasmic or apoplasmic pathways can be confidently determined (Terry & Robards, 1987; Van Bel *et al.* 1988; Warmbrodt & Van Der Woude, 1990; Russin *et al.* 1996).

There is good evidence that plasmodesmatal conductivity can be regulated by environmental and developmental signals, meaning that controlling mechanisms exist that allow the plasmodesmatal pore to dilate to allow for molecular transport (Goodwin, 1983; Turgeon & Hepler, 1989; Epel, 1994; Gamalei *et al.* 1994; McLean *et al.* 1997; Van Der Schoot & Rinner, 1999; Botha & Cross, 2000; Turgeon, 2000; Botha & Cross, 2001). There are two suggested sites and mechanisms for plasmodesmata gating, viz. the neck region by sphincters and the cytoplasmic sleeve, through actin/myosin interaction (Robinson-Beers & Evert, 1991; Badelt *et al.* 1994; White *et al.* 1994; McLean *et al.* 1997).

Sphincters, which occur in the neck regions, may be involved in the gating or regulation of intercellular traffic (Terry & Robards, 1987; Robinson-Beers & Evert, 1991; Ding *et al.* 1992; Oparka & Van Bel, 1992; Botha & Cross, 2000; Botha & Cross, 2001). Sphincters are composed of circularly spaced particles (Oparka & Van Bel, 1992), that might simply be an extension of the actin/myosin arrangement seen in the cytoplasmic sleeve (White *et al.* 1994), or could be callose-based (see Botha and Cross, 2001, and references cited).

Particles previously noted in the cytoplasmic sleeve (Robinson-Beers & Evert, 1991; Turgeon & Beebe, 1991), are now suggested to be actin, a contractile protein localized at the neck and along the cytoplasmic sleeve of the plasmodesma (White *et al.* 1994). It was hypothesized that actin/myosin interaction brings about constriction of the cytoplasmic sleeve and thus closure of the plasmodesma, and also allows for expansion to admit particles above size exclusion limit (McLean *et al.* 1997).

In 1996, Russin and co-workers suggested that a specific gene could be involved in the regulation of plasmodesmata. Although maize has numerous plasmodesmata at the interface between the bundle sheath-vascular parenchyma cells (Evert *et al.* 1977a), Russin *et al.* (1996) discovered a lack of transport at this interface in sucrose export defective1 maize mutant therefore suggesting that a specific gene associated with plasmodesmal development is involved. In phloem loading studies where ultrastructure related to transport capacity of plasmodesmata in bundle sheath-vascular parenchyma interface of non-expressing or SXD-1-expressing mutant maize leaf blade was observed (Botha *et al.* 2000), callose occluded plasmodesmata at the bundle sheath-vascular parenchyma interface were observed, and it was concluded that callose was involved in closure of plasmodesmata. There was no evidence of increased wall material deposition at or near plasmodesmatal aggregates and therefore no plasmodesmal wall occlusion mechanism was involved.

Radford *et al.* (1998) suggested that plasmodesmata could be regulated by callose deposited at the neck regions (see also Hughes & Gunning, 1980; White *et al.* 1994; Botha & Cross, 2000), due to wounding. Fluorescent dyes have been used by several authors in studying the regulation of plasmodesmata permeability by calcium and other group 2 ions (Erwee & Goodwin, 1983; Turker & Boss, 1996; Botha *et al.* 2000; Botha & Cross, 2001). Calcium has been reported to influence callose synthesis in plant cells. Callose deposits are associated with connections between cells, ranging from plasmodesmata to sieve plate pores (Currier, 1957). Increasing amount of callose could result in a slow movement of solutes and larger particles within plasmodesmata and thus plasmodesmal blockage (Erwee and Goodwin, 1983; Robards and Lucas, 1990 & references therein; Turker, 1990). Erwee & Goodwin (1983) raised cytosolic calcium concentrations within a leaf of *Egeria densa*. The leaf was first treated with F(Glu)2, a dye able to pass from cell to cell and therefore used as a probe to examine the effects of cations on symplast permeability. The results showed a decrease in the movement of dye molecules as a result of callose deposits. Schulze (1999) recently suggested that long-term high levels of calcium activate a great callose synthesis resulting in permanent closure of plasmodesmata. Blockage of plasmodesmata affect symplasmic loading and therefore a decline in symplasmic transport is observed.

There was a suggestion that inhibition of callose at plasmodesmatal neck regions are effects due to a wounding process (Radford *et al.* 1998). Botha *et al.* (2000) could not find any evidence of wounding in *Zea mays* SXD-1 mutant leaf blade tissue. In tissues where lucifer yellow transport was inhibited at the bundle sheath-vascular parenchyma interface, callose was visible immediately after addition of aniline blue. In sections where transport was not inhibited, little or no callose deposits were observed at bundle sheath-vascular parenchyma interface up to 20 min after wounding through scraping.

Some plasmodesmata in source leaves have been suggested to become non-functional after changes from sink to source have been completed, (Turgeon, 1989) and are indicative of a symplasmic phloem unloading by the sink leaves. Evidence for this transition was provided by results of transport studies in tobacco (Turgeon, 1987; Ding *et al.* 1988) and in *Vicia faba* (Bourquin *et al.* 1990). In tobacco leaves the number of plasmodesmata between the sieve element-companion cell complex and the first layer of mesophyll cells declined in non-importing tissues to 34% of the number found in importing tissue, indicating that there is a loss of symplasmic continuity between the phloem and the surrounding cells. Consequently in *Vicia faba* leaves the frequency of plasmodesmata between the phloem and assimilating tissue was found to be markedly higher for importing veins than for exporting veins. It would appear that phloem loading is symplasmic in sink leaves of these species and apoplasmic in source leaves.

Support for the argument of plasmodesmata losing functionality, was observed in plasmodesmata between the guard cells and from guard cells to surrounding subsidiary cells in immature leaves of *Beta vulgaris* L. and *Allium cepa* L. (Willie and Lucas, 1984). However, there is some counterargument, that non-functional plasmodesmata of guard cells are eventually obliterated, while those at the sieve element companion-complex border are retained. Cognisance must therefore be taken of the fact that plasmodesmata as seen at the EM level are merely snapshots in time (Robards and Lucas, 1990) and have been argued not to give a true reflection of symplasmic capacity, but simply serve as indicators of a potential symplasmic pathway (Botha and Van Bel 1992).

1.4 Symplasmic loading versus apoplasmic loading

Since the work of Geiger and co-workers in sugar beet in the 1970's it has been widely accepted that phloem loading can occur directly from the apoplast (Geiger, 1975; Giaquinta, 1983; Delrot, 1989). However, some authors have recently criticized the experimental approaches that led to this conclusion, and have suggested that phloem loading might equally be symplasmic. Some evidence for an apoplasmic mode of phloem loading came from experiments involving the structure of the phloem loading pathway and plasmodesmatal frequency studies. That the thin-walled sieve tubes have abundant plasmodesmata with their companion cells but few with other cells was thought to support apoplastic loading.

Evert and Russin (1993) argued that, based on structure, phloem unloading in the maize leaf cannot be symplasmic. These authors focused on the protophloem sieve tube, which is the first sieve tube to mature in importing bundles. Based on anatomical studies, they discovered that both the protophloem sieve tubes and the later-formed thin-walled metaphloem sieve tubes and their associated companion cells (the sieve tube-companion cell complex) have few plasmodesmatal connections with other cell types and therefore are virtually isolated symplasmically from the rest of the leaf, precluding a symplasmic mode of phloem unloading.

Evidence for symplasmic loading was demonstrated by Evert *et al.* (1977a) in plasmodesmata between vascular parenchyma cells and bundle sheath cells and between bundle sheath cells and the mesophyll cells in maize plants. Ultrastructural evidence in *Z. mays* indicates that these plasmodesmata are constricted by suberin lamellae. Suberin lamella have been demonstrated to act as a barrier to apoplasmic movement of ions between bundle sheath and mesophyll cells and thereby forcing adoption of a more regulated symplasmic pathway (Läuchli, 1976; Evert *et al.* 1977a; Evert *et al.* 1985; Botha and Evert, 1986; Botha, 1992 and references therein).

The presence of starch in mesophyll cells can also be taken as an indication of a symplasmic mode of phloem loading (Oparka and Van Bel, 1992; Gamalei *et al.* 1994; Russin *et al.* 1996; Van Bel, 1996). Apoplasmic loaders have very little in the way of starch deposits (Oparka and Van Bel, 1992).

Some previous evidence for the existance of a symplasmic mode of loading was obtained in dicotyledonous species in which a comparison of uptake into leaf discs of *Pisum sativum* (transfer cells in the minor vein phloem) and *Coleus blumei* (intermediary and ordinary companion cells) was carried out (Turgeon and Wimmers, 1988). These species are of different systems, *Pisum* being a type-2 plant and therefore using a polymer-trapping model to load its assimilates, and *Coleus* being a type-1 species with abundant connections between the complex and other cells. It was found out that *Pisum* loaded sucrose into the veins within 1min as expected if it were loaded from the apoplast. In *Coleus*, exogenous sucrose took longer to arrive at the ST/CC complexes. This was due to an inability of ST/CC complexes to load directly from the free space, requiring the absorbed sucrose to travel through the mesophyll first. Therefore the absence of direct vein loading of sucrose from the apoplast strongly suggests that the *in vivo* pathway is through the symplast (see also, Madore and Webb, 1981 for *Cucurbit*; Van Bel and Koops, 1985 for *Commelina*). Furthermore, Schmitz *et al.* 1987 also provided some evidence of symplasmic loading by feeding mesophyll tissue of *Cucumus melo* with ^{14}C. Their (Schmitz *et al.* 1987) studies demonstrated an *in vivo* path of the ^{14}C labeled photosynthates from the mesophyll to the sieve tube.

Additional evidence for the symplasmic mode of phloem loading has also been obtained from investigations using metabolic inhibitors such as PCMBS (Madore and Lucas, 1987; Weisberg *et al.* 1988; Bourquin *et al.* 1990; Turgeon and Gowan, 1990; Turgeon *et al.* 1993; Flora and Madore, 1996; McLean *et al.* 1997). PCMBS has been shown to reduce phloem symport activity in phloem membranes (Giaquinta, 1979). PCMBS has demonstrated unequivocally a relationship between the minor vein configuration and the mode of phloem loading (van Bel *et al.* 1992). For example, *Ipomaea tricolor* leaves (Madore and

Lucas, 1987) showing symplasmic continuity using fluorescent dyes, and with plasmodesmatal connections from the mesophyll to the companion cell-sieve element were treated with PCMBS. Treatment with this impermeable reagent did not show any effect on the movement through the symplasm and therefore a continuous symplasmic movement of Lucifer yellow from the mesophyll to the minor vein. In the case of apoplasmic loading, one would expect such inhibitors to interfere with the sieve tube loading.

If the argument for symplastic transport is based upon plasmodesmatal frequency studies alone, then their presence suggest the possibility of movement via the symplast but does not allow us to conclude that it necessarily occurs (Farrar *et al.* 1992). Several authors have suggested that reliance upon the plasmodesmatal frequency alone as a determinant of cell-to-cell transport (see Botha and van Bel, 1992; van Bel and Oparka, 1995; Botha and Cross, 1997) should be treated with caution when interpreting results. Botha and van Bel (1992) argued that plasmodesmatal frequency data merely gave an indication of the maximum potential pathway of symplasmic transport and do not take the transport capacity into account.

1.5 The use of fluorescent tracers in phloem loading

Fluorescent dyes such as Lucifer yellow (LYCF) and 5,6-carboxyfluorescein diacetate (5,6-CFDA), have provided a great deal of useful information about the symplasmic continuity in living plant tissues. These fluorochromes have been used extensively in plant research as markers for symplasmic transport (Grignon *et al.* 1989; Oparka, 1991; Oparka *et al.* 1994; Wright and Oparka, 1996; Roberts *et al.* 1997). The hydrolysed products of these fluorochromes are unable to move through the plasmalemma (Stewart, 1981; Goodwin, 1983; Miller *et al.* 1983; Erwee *et al.* 1985; Terry and Robards, 1987), and must be transported via the plasmodesmata. Movement of dyes within plants suggests cell-to-cell movement of solutes *in vivo*. If the dye is injected into a single cell and is then seen in others, this provides direct evidence of symplasmic continuity between these cells via plasmodesmata (Turker *et al.* 1989; Farrar *et al.* 1992). Fisher (1988) carried out dye coupling experiments with *Coleus blumei*. Injecting lucifer yellow in the mesophyll cells of this plant, showed that the dye moved to the adjacent mesophyll cells, and often into the bundle sheaths for some distance away from the site of injection, therefore providing evidence that plasmodesmata connecting these cells were undoubtedly functional. It is not only the presence of plasmodesmata that is a regulatory factor for symplasmic continuity, but also their frequency. Terry and Robards (1987) have shown that the time required for fluorescent dyes to reach the threshold of detection in the cell adjacent to the injected one is not only dependent on the size of the pore opening, but also on the number of the plasmodesmata connecting those cells.

Erwee *et al.* (1985) demonstrated that molecular dyes injected in the leaf of *Commelina cynae* could move to the vascular bundle and that subsequent movement takes place preferentially along the minor vein. Consequently, studies taken by Madore *et al.* (1986) also showed that fluorescent dyes injected in the mesophyll cells could move along the minor vein phloem. Although the movement along veins in these species was observed, attempts to locate the dye within the sieve elements proved to be difficult. Fluorescent dye injected in the mesophyll cells of *Commelina benghalensis* (Van Kesteren *et al.* 1988) was monitored and the dye movement allowed the identification of the exact pathway followed by the dye. The dye moved between mesophyll cells as well as through the mestome sheath into the sieve tubes. Subsequent studies with *Cucurbita pepo* (Turgeon and Hepler, 1989) supported these results whereby the abaxial phloem of these veins was exposed by stripping the lower epidermis and removing the spongy mesophyll cells by abrasion. Fluorescent dyes were microinjected into intermediary cells by iontophoresis and the dye transfer was observed. The dye spread from one intermediary cell to the other and from intermediary cell to the bundle sheath and mesophyll cell as well as through mestome sheath into the sieve tubes, suggesting that photoassimilates are loaded from the mesophyll cells to the sieve tube in the minor vein phloem. It is clear from the preceding that the use of symplasmically-transported fluorescent dyes, has revealed the pathways followed by these fluorochromes from the mesophyll to sieve tube, and this is possible through functional plasmodesma.

1.6 Increases in atmospheric carbon dioxide (CO2) related to phloem loading

Maize has a high rate of photosynthesis (Kalt-Torres *et al.* 1987), which requires that assimilated carbon be rapidly transported to the bundle sheath cells, where malate decarboxylation and assimilation of the carbon into sucrose occurs. Most of the photosynthate is rapidly transported via plasmodesmata down a symplasmic gradient and eventually uploaded to the phloem where it is assumed to be loaded apoplasmically into the sieve-tube members of the small bundles. Some of the photosynthates are accumulated as starch in the chloroplasts of the mesophyll cells, where they are metabolized further during the subsequent dark period.

Predictions that atmospheric carbon dioxide concentrations will continue to increase into the next century have prompted extensive research into effects of climate in crop production (Cure and Acock, 1986; Lawler and Mitchell, 1991; Conroy *et al.* 1994; Woodrow, 1994). Increases in atmospheric carbon dioxide result in increases in photosynthetic carbon fixation, and thus increases in carbohydrate accumulation particularly starch within the source leaves (Apel, 1976; Cave *et al.* 1981; Preiss, 1982; Thomas and Harvey, 1983; Cure and Acock, 1986; Vu *et al.* 1989; Bowes, 1991; Lawler and Mitchell, 1991; Madsen, 1968; Stitt, 1991; Wolfe and Erickson, 1993; Conroy *et al.* 1994; Kutik *et al.* 1995; Pritchard *et al.* 1997). This simply means that doubling atmospheric carbon dioxide levels potentially doubles the carbon available for carbohydrate production during photosynthesis. Starch accumulation is an important buffering component for carbohydrates allowing a continuous export of assimilates (Heineke *et al.* 1999) thus facilitating fast growth particularly under varying light conditions.

1.7 Objectives

Whether the pathway followed by photosynthate from the mesophyll to the sieve tube of grass leaves is symplasmic or apoplasmic or includes both possibilities, continues to be the subject of recurrent discussion. Few of the phloem loading studies carried out in grasses (especially in maize) have only dealt with plasmodesmatal frequencies. It is only Haupt *et al.* (2001) who has been successful in determining the phloem unloading pathway in barley leaves using the membrane impermeant dye, 5,6-CF. Therefore this study explores the loading pathway in maize leaves exposed to ambient and elevated CO_2 using the membrane impermeant dye, 5,6-carboxyfluorescein (5,6-CF).

It has been suggested that for wheat leaves, lateral transfer of assimilates from the small into the larger veins occurs via the cross vein, (Altus and Canny, 1982, 1985; Evert, 1986). Therefore this research also focuses attention on the transfer of 5,6-CF from loading to the transporting veins via the interconnecting cross vein system in maize leaves and also to observe if the sieve tube of the cross vein is involved in lateral transfer of 5,6-CF from one longitudinal vein to the other.

Matsiliza and Botha (2002) provided the first evidence on preferential feeding of the aphid, *Stobion yakini* from the thin-walled sieve tubes of barley. The study suggested that thin-walled sieve tubes could be more functional than the thick-walled sieve tubes.

Based on the information presented on the introduction several questions arise that form the basis of the research reported here.

(1) Is transport capacity under elevated carbon dioxide enhanced or not?

(2) Does a symplasmic uptake pathway exist from the mesophyll cell to the sieve tube?

(3) Which sieve tubes (i.e., thin- or thick-walled or both) are functional in the loading and unloading process in the maize leaf?

(4) Are there any connections between the sieve tubes of the cross vein and those of the longitudinal veins?

(5) Can 5,6-CF be loaded directly from the apoplast?

This thesis focuses attention on the loading and transport pathways in source and sink leaves in *Zea mays* grown and maintained under normal and elevated CO_2 conditions under dark and in light conditions.

CHAPTER 2: MATERIALS AND METHODS

2.1 Plant Material

Maize seeds (*Zea mays* L. var. Early Pearl) were obtained from Agricol, Paarl Road, Brackenfell, South Africa. Seeds were soaked in water overnight and pre-germinated in Petri dishes in an incubator at a temperature of 15 ^{0}C. Germinated seeds were planted in potting soil (Greenfingers, Port Elizabeth, South Africa) and plants grown in a greenhouse at temperatures between 15 and 35 ^{0}C. Seedlings, 4- to 6- day-old plants were placed in E10 controlled environment cabinets (Conviron, Controlled Environments Ltd. Winnipeg, Canada) at 200 $\mu mol.m^{-2}\ s^{-1}$. The plants were watered two to three times a week with 50% Long-Ashton nutrient solution (Appendix A, Hewitt 1966). These plants were exposed to two different carbon dioxide concentrations. One group of plants was grown at a carbon dioxide concentration which was maintained at ambient CO_2 levels (ca 375 ppm) and the other group was grown at elevated CO_2 maintained between 650 and 700 ppm. The temperatures in both cabinets were maintained at 27 ^{0}C during the day and 24 ^{0}C during the night. The relative humidity was set at 60% during the day and 50-55% during the night to maintain constant saturated vapour pressure deficit in the cabinets and the irradiance was set at 200 $\mu mol\ .m^{-2} s^{-1}$.

2.2 Sampling Procedure

Plants used were taken either from the cabinet kept at ambient CO_2 or the cabinet treated with elevated CO_2. Source leaves approximately 20 cm long were taken from 40 day-old-plants and sink leaves approximately 9 cm, from 14 day-old-plants. The 3rd visible leaf was used in all sink leaf experiments and the 5th leaf counting from the top was used for all the source leaf experiments.

2.3 Light microscopy

Leaf segments were fixed in Formalin-acetic acid alcohol (FAA) for 24 hours (Table 2). The leaf segments were dehydrated through an alcohol and tertiary butyl alcohol series (Table 1) and then infiltrated with liquid paraffin and 3 changes of Paraplast wax over 3 days, in an embedding oven at 60 ^{0}C. Blocks were mounted and trimmed to enable cutting of paradermal and transverse sections at 13-15 μm using a Minot rotatory microtome (Leitz Wetzlar, Germany). Sections were dewaxed in 3 changes of xylol and stained in safranin and fast green (Table 3). The stained sections were then mounted under long coverslips (Superior, Chance proper Ltd, West Germany) using Canada Balsam. Mounted slides were then hardened in an oven at 47 ^{0}C for three weeks, prior to examination.

2.4 Fluorescence microscopy

2.4.1 Aniline blue fluorescence microscopy

Aniline blue WS (GT Gurr, London, England) was made up as a 0.05% (w/v) solution in distilled water. Leaf strips approximately 5 mm x 3 cm were mounted on glass slides and were gently scraped on the abaxial side and stained with aniline blue under 0.1 M MES buffer solution. After 10 minutes the leaf strips were examined for the presence of callose and photographed on a Standard Zeiss Junior 18 epifluorescence microscope using either a Plan-neofluar X25 (numerical aperture, 0.8) or X40 (numerical aperture, 0.9 oil/glycerine/water immersion), objective lens. High resolution digital images were captured using an Olympus DP-10 camera (Olympus, Japan), fitted to the microscope. A Chroma 1103 blue/violet filter set (Excitation: 425-440 (BP); Emission: 475nm; (LP), 460 DCLP) was used for all images taken. Images were stored for later manipulation as tagged image file format (TIFF) files.

2.4.2 Leaf tissue preparation for 5,6 Carboxyfluorescein (5,6-CFDA) application

Five and six carboxyfluorescein (5,6-CFDA) was purchased as the diacetate (5- and -6) CFDA, mixed isomers from Molecular probes, Leiden, The Netherlands, catalogue number C-195). It has a chemical formula of C_{25} H_{16} O_9 and the molecular weight = 460.40 and its molecular structure is given below.

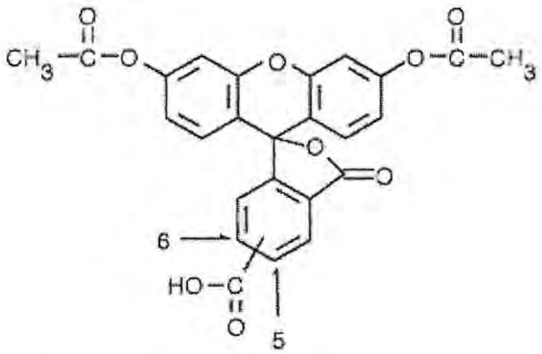

Five and six Carboxyfluorescein was made up as follows: 100 mg of 5,6-CFDA was added to 1 ml DMSO to make a stock solution and then 1-5 μl of the stock solution was diluted to 5 ml of distilled water. Experiments were carried out using plants that were dark adapted, as well as plants that had been maintained in the light at 200 μmol m^{-2} s^{-1}. A part of an attached leaf was gently scraped and abraded under MES buffer with a sharp single-edged razor blade to remove the cuticle and the epidermal tissue from the abaxial surface (effectively opening 'windows' into the mesophyll), in regions into which 5,6-CFDA was introduced intracellularly. After 3 h leaf strips (about 3 mmx5 cm) were cut from the leaf and its epidermis was gently scraped on the abaxial surface on a glass slide under MES buffer and placed under a coverslip. The symplasmic transfer of the dye within the leaf strips was examined using a Zeiss Standard Junior 18 epifluorescence microscope and the photographs were taken in the same manner as for microscopic examination for aniline blue. All the images were taken using a Chroma Yellow GFP BP 10C/Topaz filter set # 41028 (Chroma Technology Corp, Battleboro, VT, USA).

2.4.3 Aniline blue and 5,6-CFDA fluorescence microscopy

The attached leaves were gently scraped as for leaf tissue preparation for 5,6-CFDA and the dye was introduced through the abraded leaf surface. After 3 h leaf strips approximately 5 mm x 5 cm were removed from the plant. The abaxial interface was scraped gently to remove the epidermis and then mounted in 0.05 % (w/v) aniline blue solution and immediately observed using a Standard Junior 18 Zeiss microscope fitted for epifluorescence microscope using 25X and 40X water-immersion optics. High resolution images were captured using an Olympus DP-10 camera (Olympus, Japan), fitted to the microscope.

2.4.4 Preparation of Texas Red

Texas Red (chemical formula =$C_{31}H_{30}N_2O_7S_2$; molecular weight =606.71; sulforhodamine 101 catalogue number S5138, Sigma Aldrich Chemical Corp, Sigma, Atlasville, South Africa). The molecular structure is given below.

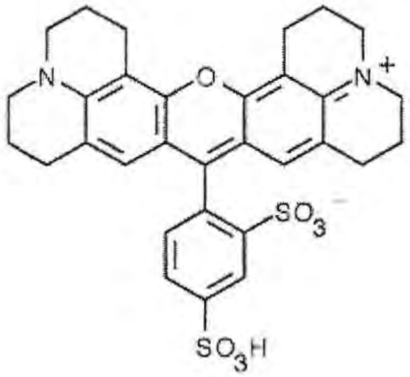

Texas Red is an apoplasmically-transported molecule, thus could be used to illuminate the apoplast (cell walls and free space). The stock solution was made up using 25 mg in 1.0 ml distilled water, and working solution was made up using 25 mg in 1.0 ml distilled water, and working solutions were prepared by diluting 1-2 µl stock into 1.0 ml distilled water (final concetration 0.04 mM).

2.4.5 Uptake of 5,6-CFDA and Texas Red via the transpiration stream

Six-to-eight-cm-long leaves, were immersed in a vial which contained 5,6-CFDA, which was taken up in the transpiration stream. And after 120 and 180 min, the whole leaf was removed from the vial and examined immediately using the epifluorescence microscope. Transections of regions of interest (i.e., where strong 5,6-CF fluorescence was seen) were cut at 15-25 µm into silicone oil using a Mclwain Tissue Chopper (The Mickle Laboratory Engineering CO. Ltd. Gomshall, Surrey). These sections were mounted on slides under silicone oil and observed using the Zeiss epifluorescence microscope and examined using the Chroma Topaz filter set which excluded lignin autofluorescence from the images. Some of the leaves were immediately transferred to a vial containing a working solution of Texas Red for 60min. These were examined to co-localize the Texas Red and 5,6-CFDA fronts before being cut at 15-25 µm into silicone oil using a Mclwain Tissue Chopper. All the images were taken using a filter set specific for 5,6-CFDA and for Texas Red, TRC # 31004 and combined images were taken and manipulated using the *m*-Fip routine from SiS (Soft Imaging System GmbH., Münster, Germany).

2.5 Digital imaging

Imaging was achieved using either Zeiss Standard 18 or Olympus BH-2 (Tokyo Japan), using an Olympus DP-10 digital camera, or a Colorview XS Peltier-cooled camera (Soft Imaging System, (SiS GmbH. Münster, Germany). For the Olympus DP-10 digital camera, selected images were taken at 1280 X 1024 pixels per inch resolution with Olympus CW-95 Software, and the images were captured as tagged information format (TIFF) files. For the Colorview XS Peltier-cooled camera, TIFF images were captured and manipulated using the SiS version 3.2 (build 731) software package.

CHAPTER 3: RESULTS

3.1General anatomy of the maize leaf

Figure 3.1 is the plate showing the vascular bundles of a maize leaf as viewed in transverse (Fig 3.1A & B) and paradermal (Fig 3.1C-F) sections. Typical monocotyledonous features were observed as discussed in the introduction. The different bundle orders were always connected by the transverse vein (Fig 3.1; Evert *et al.* 1978). Fig 3.1A shows a portion of the cross vein connecting to the longitudinal vein, with the cross vein sieve tube directly connected to the small thin-walled sieve tube of the longitudinal bundle located near the xylem (Fritz *et al.* 1989). The phloem contains no fewer than two sieve tubes, thin- and thick-walled sieve tube, companion cells and parenchyma cells (Fig 3.1A; see also Evert, 1980 & references cited therein). Thin-walled sieve tubes are always associated with two or more companion cells and thick-walled sieve tubes closely associated with one or more xylem vessels. Some parenchyma cells were associated with phloem and xylem and because they were similar cytologically, they were designated as vascular parenchyma cells (Botha & Evert, 1988).

Fig 3.1B shows a transverse vein connection between a small (collecting) and a large (transporting) bundle. Sieve plates were definite within the sieve tube of the cross vein (arrowheads). This sieve tube of the cross vein is connecting to the position of the thick-walled sieve tube of the large bundle, as suggested by literature (Evert, 1986).

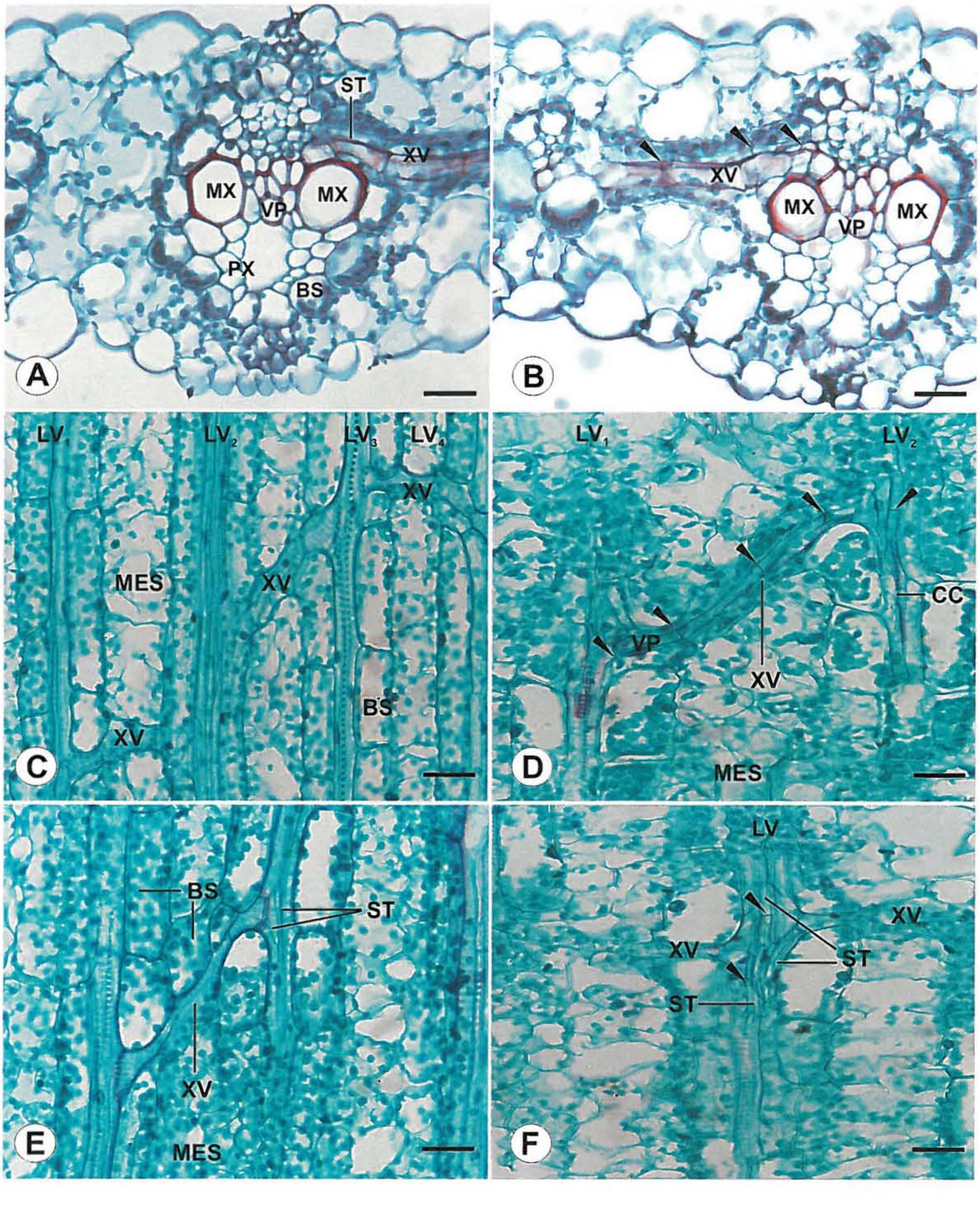
ST
XV
MX
VP
MX
PX
BS
A
XV
MX
VP
MX
B
LV$_1$
LV$_2$
LV$_3$
LV$_4$
XV
MES
XV
BS
XV
C
LV$_1$
LV$_2$
CC
VP
XV
MES
D
BS
ST
XV
MES
E
LV
XV
XV
ST
ST
ST
F

Fig. 3.1 (A-F): detailed anatomical structures of a maize leaf taken from transverse (Fig. 1A-B) and paradermal sections (Fig.1C-F) using a light microscope. **A** shows details of the phloem tissue in a large vein and a portion of the cross vein connecting to the thin-walled sieve tube of this vein. **B.** shows a cross vein connection between the small and the large vein. The sieve tube shows sieve plates (arrowheads) and the sieve tube of the cross vein connecting at the position of the thick-walled sieve tube. **C.** shows a typical pattern of the leaf blade, cross veins connecting to the longitudinal bundles taken at the level of the phloem. **D.** details of the cross vein sieve tube showing four sieve tube members connected by sieve plates (arrowheads). Also showing a little portion of the longitudinal bundle sieve tube with sieve plates too (arrowheads). **E.** shows the cross vein sieve tube joining that of the longitudinal vein at the cross vein junction. The cell adjacent to the elbow could be a thick-walled sieve tube. **F.** shows in detail the organization of the cells at the cross vein junction. The cross vein sieve tube is observed joining the longitudinal vein downwards. Note the evidence of two sieve tubes within the longitudinal vein as identified by sieve plate.

BS= bundle sheath; VP= vascular parenchyma; MES= mesophyll; LV= longitudinal vein; XV= cross vein; MX= metaxylem; PX= protoxylem; ST= sieve tube; TWST= thick-walled sieve tube; STM= sieve tube member; CC= companion cell; dotted further = zone of the phloem; cells with a black dot appearance = thick-walled sieve tube; cells without a black dot appearance = thin-walled sieve tubes; small cells alternating with the thin-walled sieve tubes = companion cells. (A-F) Bars =10μm

Figure 3.1C is a paradermal section taken at the level of the phloem which shows a typical vascular pattern and lateral interconnections between the vascular bundles in *Zea mays* leaf. In some cross veins, the vascular bundle-sheath cells varied from absent to entire (see also Evert *et al.* 1978). There are always never more than two rows of mesophyll cells between adjacent bundle-sheath cells (Evert *et al.* 1977a). Some of the transverse veins are lying at right angles to their associated longitudinal veins while others extend obliquely between them.

Fig 3.1D shows a higher magnification view, showing a cross vein. The sieve tube of the cross vein is made up of four sieve tube members joined end to end by sieve plates (arrowheads). At the junction of the cross vein, the sieve tube of the cross vein joins the longitudinal bundle (LV1) downwards and next to the observed tracheids. The other longitudinal vein shows three sieve plates and therefore two sieve tube members indicating the presence of a sieve tube. It is between this sieve tube and the vascular parenchyma that another cell was observed and possibly, the companion cell. The bundle sheath was not entire in this vein.

Fig 3.1E shows the connection of the cross vein sieve tube to that of the longitudinal vein. The sieve tube of the cross vein joins that of the longitudinal vein (LV2) and adjacent to this a thick-walled sieve tube was observed. This vein shows a continuous bundle sheath surrounding the cross vein.

Fig 3.1F shows a small longitudinal vein and the junction of the phloem of the longitudinal vein with the cross vein. The cross vein joining the longitudinal bundle contained one sieve tube and several were apparent within the longitudinal vein via sieve plates (arrowheads). Both of these longitudinal vein sieve tubes are joined by the sieve tubes emerging from either side of the cross veins.

3.2 Transport studies

3.2.1 Visualization of the aniline blue-stained callose deposition

Aniline blue was applied to lightly scraped leaf sections, immersed in water, to visualize the deposition of callose in plasmodesma, pore plasmodesmal units and between companion cells and their associated sieve tube members, and also to highlight callose associated with sieve plates.

Fig 3.2 (A-D) shows fluorescence images taken from a leaf blade tissue 10 min after aniline blue staining to reveal callose deposition associated with the phloem. In Fig 3.2A heavy callose deposits were observed associated with the sieve plates (arrowheads) in the cross vein connecting the two longitudinal veins, and also within the longitudinal veins. Note that the cross vein contains only one sieve tube, which is a thin-walled sieve tube, and is composed of four sieve tube members, joined end to end by brightly fluorescing sieve plates. The upper of the four sieve tube members shows symplasmic connections with either a phloem parenchyma or companion cell. Note callose deposits associated with pore plasmodesmatal units fluorescing between the sieve tube and their associated companion cells (short arrows). The other smaller punctuate deposits highlighted by callose in other vascular tissues are plasmodesmatal fields. Note that the sieve tube of the cross vein is clearly visible joining that of the longitudinal vein at the junction of these veins.

Fig 3.2B shows the small longitudinal vein (LV2) showing aggregates of plasmodesmata highlighted by punctate callose deposits in the boundary between the vascular parenchyma and the bundle sheath cells and also pore plasmodesmatal units fluorescing between the vascular parenchyma and the phloem (short arrows). Note the brightly-fluorescing callose deposits at the sieve plate pore sites within the small longitudinal vein as well as the single sieve plate highlighted within the intermediate vein (arrowheads).

In Fig 3.2C, callose deposits can be seen associated with the sieve plate pores (arrowheads) within the cross vein and the small longitudinal bundles. The cross vein is made up of three sieve tube members joined end to end by the sieve plates. Of interest in this image is the observed fluorescing and non-fluorescing callose deposits between the sieve tube and the vascular parenchyma (see, LV2). The sieve tube of the longitudinal vein showed one sieve tube member identified by callose deposits at sieve plate pores.

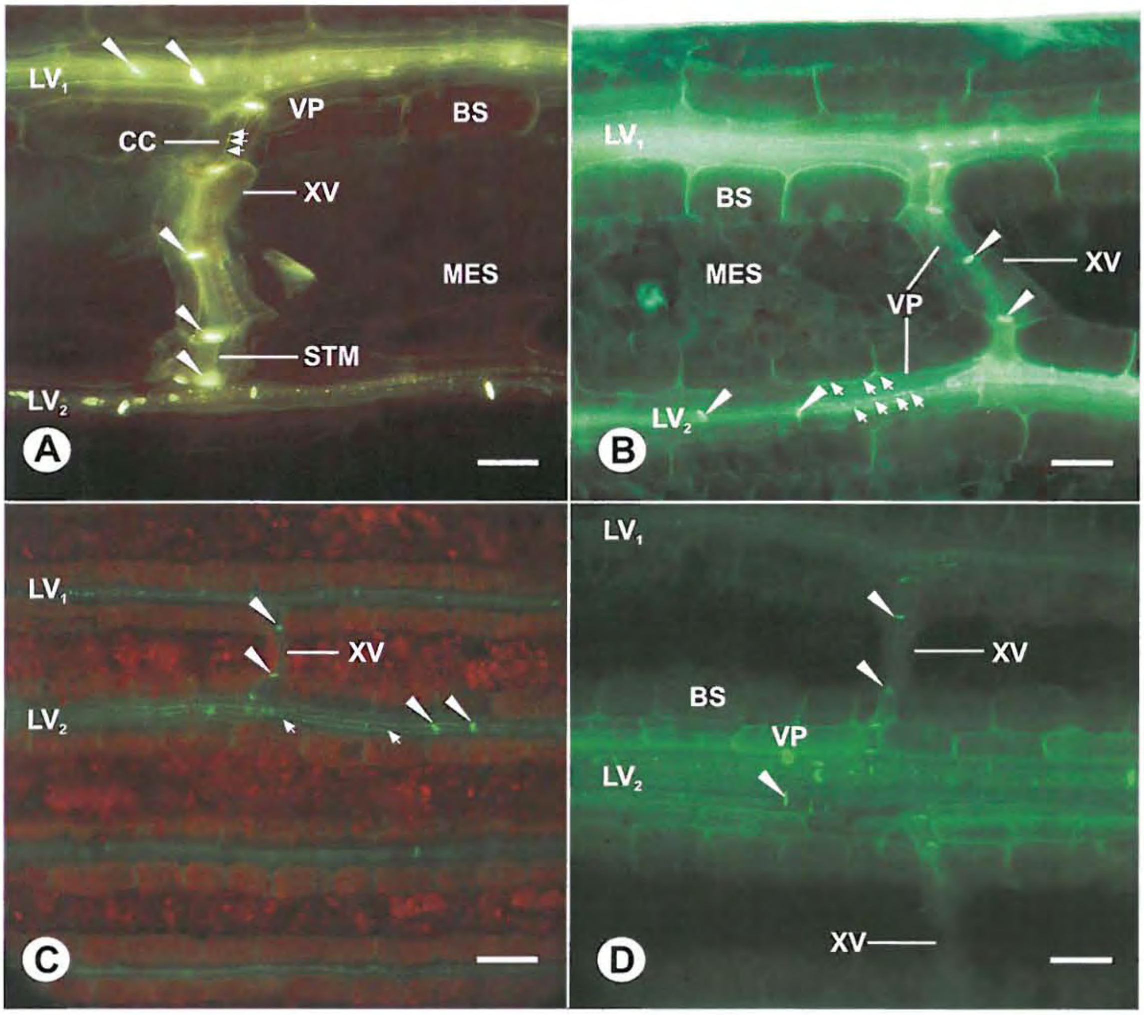
LV1
VP
BS
CC
XV
MES
STM
LV2
A
LV1
BS
MES
VP
XV
LV2
B
LV1
XV
LV2
C
LV1
XV
BS
VP
LV2
XV
D

Fig 3.2: shows images taken from sink leaf tissues after 10min of aniline blue staining, showing the distribution of callose in the cells of the phloem. **A** shows bright callose deposits associated with sieve plate pores in the longitudinal bundles and in the cross vein (arrowheads). A. single sieve tube composed of four sieve tube members. Smaller punctate deposits are pore plasmodesmatal between the companion cell and the sieve tube (short arrows), and the faint fluorescence is associated with plasmodesmatal fields within the phloem. **B.** shows two small longitudinal veins interconnected by the cross vein. Fluorescing callose-occluded sieve plates are observed in the cross vein and the longitudinal veins (arrowheads). Fluorescing callose deposits are associated with plasmodesmatal aggregates and pore plasmodesmatal units between the vascular parenchyma and the bundle sheath, and between the vascular parenchyma and the phloem, (short arrows). **C.** shows two small longitudinal veins connected by a cross vein. The cross vein contains three sieve tube members. Note the observed sieve tube member of the longitudinal vein (LV2). Pore plasmodesmatal units are fluorescing between the sieve tube and the vascular parenchyma. **D.** shows two emergent cross veins associated with a large longitudinal bundle. Bright callose deposits are associated with sieve plate pores (arrowheads). The cross vein connecting the two longitudinal veins shows four sieve tube members. Bright punctate deposits observed within the large vein are associated with pore plasmodesmatal units. Note that the thin-walled sieve tube of the cross vein is clearly visible joining that of the longitudinal vein at the junction of the cross vein (see, LV1).

LV= longitudinal vein; XV= cross vein; BS= bundle sheath; VP= vascular parenchyma; MES= mesophyll; STM= sieve tube member; CC= companion cell; arrowheads= sieve plates; short arrows= pore plamodesmatal units. (A-D) Bars = 10μm

Fig 3.2D shows callose deposits associated with the sieve plate pores (arrowheads) within the sieve tubes of the large longitudinal bundle and within that of the associated cross veins. Note that the cross vein emerging from the top is composed of four sieve tube members and only one sieve tube member was possibly visualized within the cross vein emerging from the bottom. The other bright, and some faint punctate deposits observed within the longitudinal vein, are associated with multiple pore plasmodesmatal units at the companion cell-sieve tube interface (short arrows).

The experimental approach using aniline blue made it relatively easy to identify the cells associated with the phloem via callose deposits. Callose deposits at sieve plate pore sites allowed identification of the sieve tubes within the longitudinal bundles and the cross veins. Cross veins are composed of only one sieve tube and are associated with parenchymatic elements including companion cells (clearly visible in Fig 3.2A). In contrast to Evert *et al.* (1978), the bundle sheath seem to be entire in many of the sections I looked at. Perhaps this differs in different varieties. Clearly the cross veins appeared to contain only one sieve tube, and that this sieve tube appeared to be a thin-walled one (companion cell-like cells were seen). Transport of 5,6-CF, if evident via the cross veins would suggest a symplasmic role for the thin-walled sieve tubes.

3.2.2 Visualization of the fluorochrome (5,6-CF) transport within sink leaves

5,6-carboxyfluorescein was introduced into the symplast of sink leaves maintained at ambient and elevated carbon dioxide as described in the materials and methods. Each leaf was observed 3 h after the application of the fluorochrome and the results obtained were similar.

Fig.3.3 shows an example of the results obtained from one of the ten experiments for the leaf tissue exposed to ambient CO_2 and the images demonstrate evidence of a typical offloading sequence within a sink leaf. On examination of the leaf strip, longitudinal acropetal transport of the fluorochrome from the point of loading was observed, approximately 3cm from the point of application. Fig. 3.3A was taken in the region of application and Fig. 3.3D is at approximately 3cm away from the point of application.

Intense fluorescence was observed within the vascular parenchyma and in the phloem with little fluorescence shown within the bundle sheath and the mesophyll cells respectively (Fig 3.3A). Approximately 1 cm from the point of application (Fig. 3.3B), more intense 5,6-CF fluorescence was visible within the vascular parenchyma (see, LV1) and within the phloem (see, LV2). Note that the bundle sheath cells show an increase in 5,6-CF-associated fluorescence. Of the three longitudinal bundles shown in this image, two small veins (LV1 & 2) were connected by a cross vein. Lateral transfer of 5,6-CF was observed between

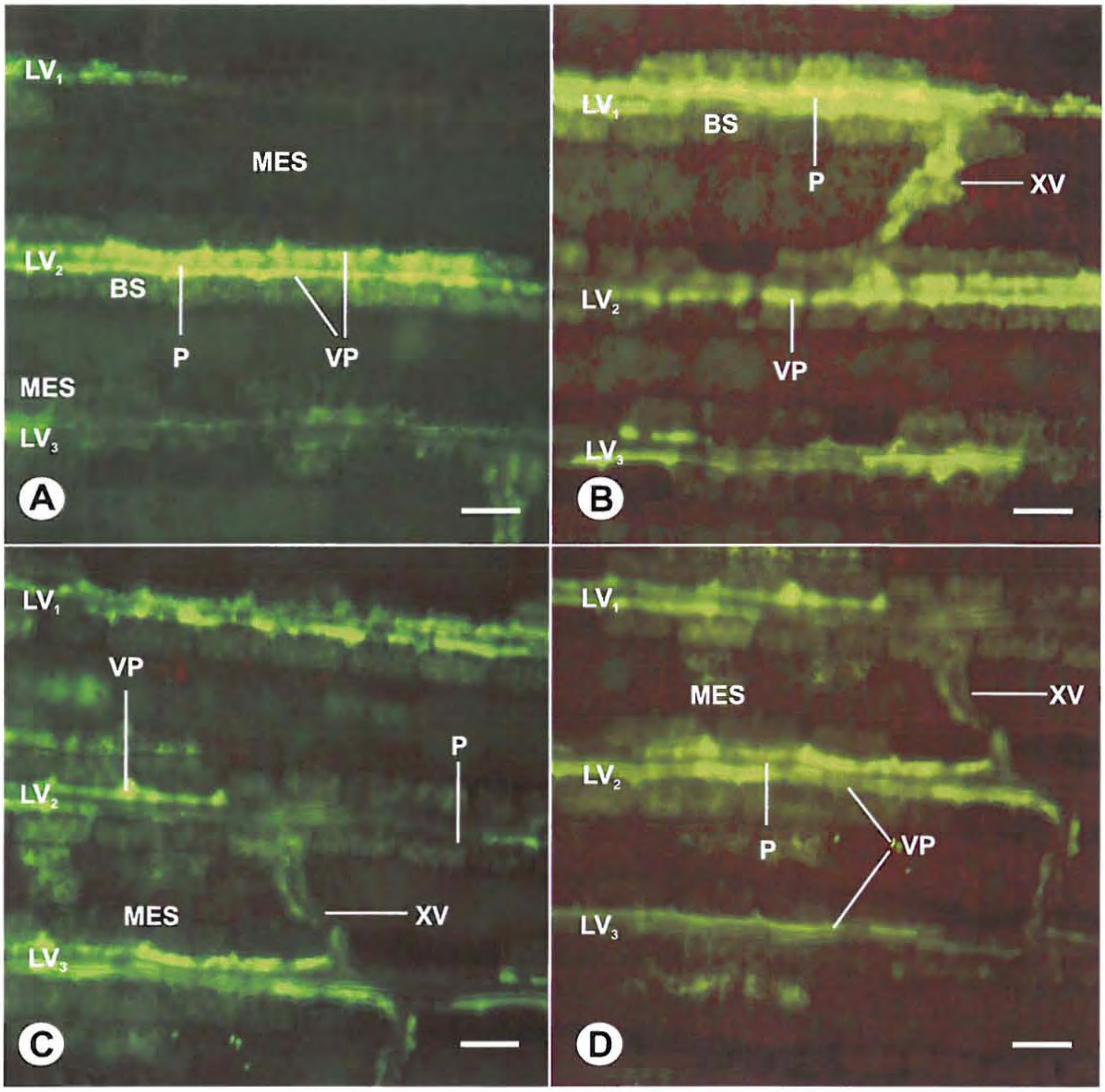
LV1
MES
LV2
BS
P
VP
MES
LV3
A
LV1
BS
P
XV
LV2
VP
LV3
B
LV1
VP
P
LV2
MES
XV
LV3
C
LV1
MES
XV
LV2
P
VP
LV3
D


3 cm
D
C
B
A
Tip
Base

Fig 3.3: Shows detail of fluorescence distribution from part of a leaf strip taken from a plant exposed to ambient CO_2, 3h after flap feeding with 5,6-CFDA showing a typical offloading sequence. The fluorochrome was introduced 4cm from the base and images were taken successively towards the tip of the leaf. Fig 3.3A is the one closest and Fig 3.3D is the furthest from the point of application. **A.** shows longitudinal acropetal transport within small veins. Less 5,6-CF-associated fluorescence was observed within the mesophyll cells except for the vascular parenchyma and the phloem. **B.** At about 1cm from the point of 5,6-CFDA application, an increase in 5,6-CF fluorescence can be seen within the vascular parenchyma. Note that lateral transfer of the fluorochrome has taken place from the small to the small or intermediate vein. **C.** image taken at approximately 2cm from the point of feeding showing increase in 5,6-CF patchiness within the vascular parenchyma. The bundle sheath and especially the mesophyll cells seem to show signs of increase in 5,6-CF fluorescence. **D.** At approximately 3cm, more intense fluorescence can be seen within the mesophyll and note that less fluorescence appears to be associated with the vascular parenchyma and the phloem.

LV= longitudinal vein; XV= cross vein; BS= bundle sheath; VP= vascular parenchyma; MES= mesophyll; P= phloem. (A-D) Bars = 20µm

these veins via the interconnecting cross vein. Fig 3.3B shows patchy distribution of the fluorochrome within the interconnected longitudinal veins and most specifically, in the vascular parenchyma and the phloem near the cross vein (see, LV1). The patchy appearance may be due to differential offloading of the fluorochrome from these cells into the bundle-sheath and then the mesophyll cells.

Fig 3.3C was taken approximately 2cm from the point of 5,6-CFDA application. Intense fluorescence was observed and within the vascular parenchyma more so than at the phloem. An increase in patchiness was seen within the vascular parenchyma of the small longitudinal vein (LV2). The vascular parenchyma of the other small vein (LV1), and the small intermediate vein, (LV3) show a slight fluorochrome increase perhaps as it is unloaded from the phloem. The bundle sheath cells show more intense fluorescence compared with the bundle sheath cells in Fig 3.3A and 3.3B, and fluorescence is evident within the adjacent mesophyll cells as well.

Fig 3.3D Illustrates the fluorescence pattern approximately 3cm from the point of application. This image seems similar to Fig 3.3C as all the cells showed 5,6-CF-associated fluorescence. Little fluorescence was observed within the vascular parenchyma and within the phloem. Clearly unloading to the mesophyll cells has occurred.

Fig. 3.4 (A-D) shows results obtained from one of the fourteen experiments for the leaf tissues exposed to elevated CO_2, and the images taken demonstrate a typical offloading sequence within a sink leaf. As in the case of the leaf material exposed to ambient CO_2, transport was acropetal. The front was observed approximately up to 5cm away from the point of application of 5,6-CFDA. Note that Fig. 3.4A is at the approximate point of application and Fig. 3.4D is at approximately 5cm away from the point of application.

Figure 3.4A is at the approximate region of application of 5,6-CFDA, and shows evidence of transport of 5,6-CF and unloading from the longitudinal veins. Of the three longitudinal veins visible, the micrograph shows two small veins (LV1& LV2) and the lowermost is an intermediate vein (LV3). LV1 shows 5,6-CF-associated fluorescence within the vascular parenchyma and along one side of the vein. Mostly, this vein shows 5,6-CF-associated fluorescence within the vascular parenchyma than in the other cells. Again, a degree of patchiness is evident here as well as in the other experiments.

In contrast, LV2 (adjacent to the intermediate vein, LV3) shows more intense 5,6-CF fluorescence within all the parenchymatic cells, including the phloem and this is especially closer to the junction of the cross vein (XV1). Patchy fluorescence can be seen in some vascular parenchyma cells and closer to the junction of the cross vein (XV2). The intermediate vein (LV3) shows bright 5,6-CF associated fluorescence within the vascular parenchyma, the phloem, and the bundle sheath

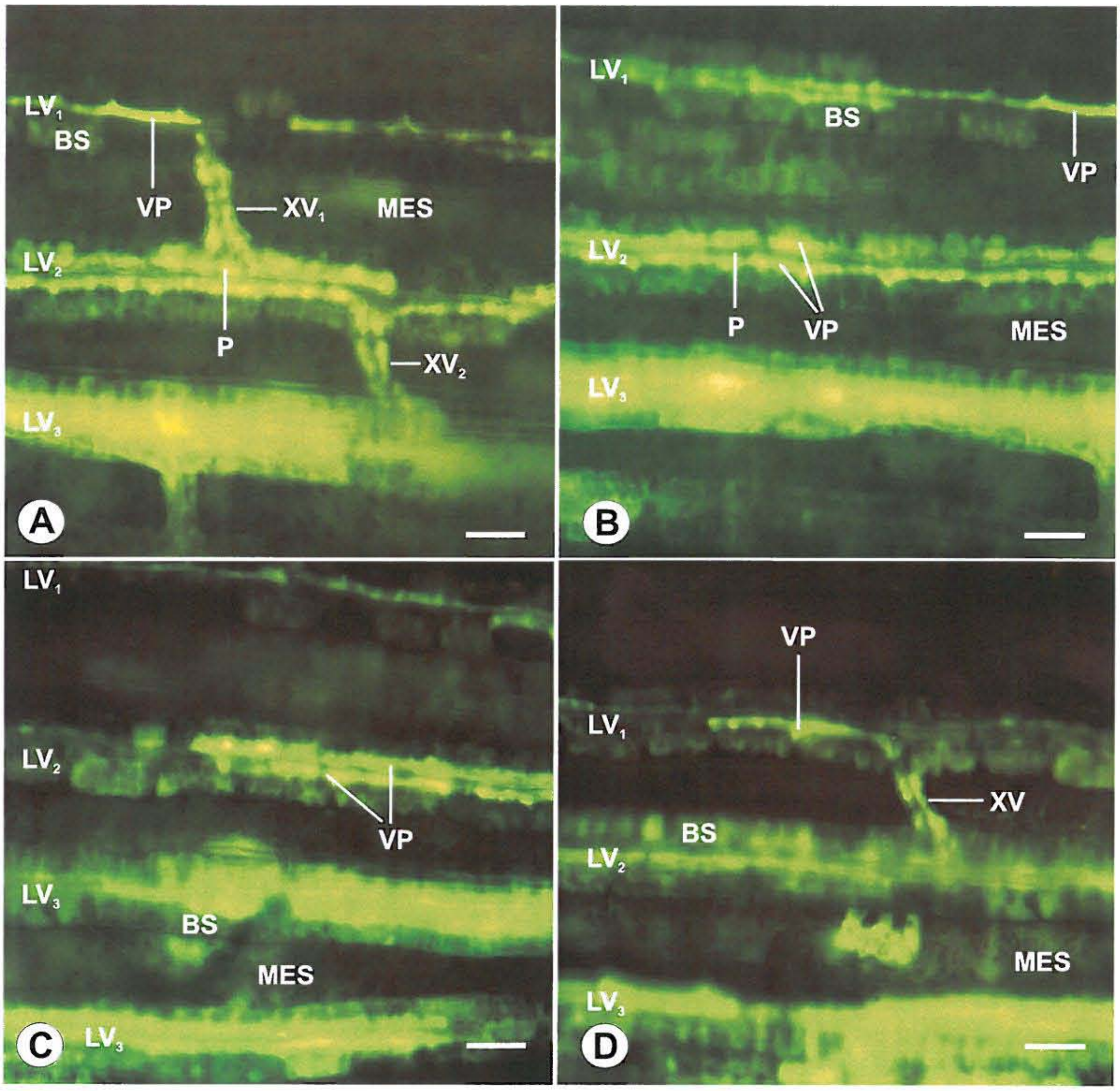
LV$_1$
BS
VP
XV$_1$
MES
LV$_2$
P
XV$_2$
LV$_3$
A
LV$_1$
BS
VP
LV$_2$
P
VP
MES
LV$_3$
B
LV$_1$
LV$_2$
VP
LV$_3$
BS
MES
C
LV$_3$
VP
LV$_1$
XV
BS
LV$_2$
MES
LV$_3$
D

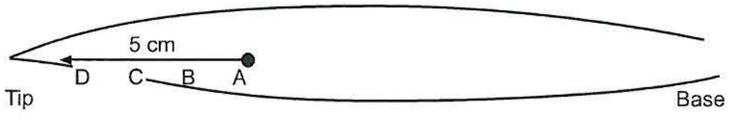
5 cm
D
C
B
A
Tip
Base

Fig 3.4: shows an example of a typical offloading sequence in selected areas of an 8cm sink leaf strip taken from plants exposed to elevated carbon dioxide after 3h of uptake of 5,6-CFDA. The fluorochrome was introduced 4cm from the base of the leaf and the images were taken successively. Fig 3.4A is in the region of application and Fig 3.4D is the furthest from the point of 5,6-CFDA application. **A.** image taken at the approximate point of introduction of 5,6-CFDA, showing two small (LV1 & LV2) and an intermediate (LV3) interconnected by the cross vein with 5,6-CF fluorescing especially within the vascular parenchyma and the phloem. LV3 shows fluorescence in all the cells except for the mesophyll. Note less fluorochrome shown within the mesophyll and the bundle sheath. The cross vein also shows 5,6- CF fluorescence. **B.** Approximately 2cm from the point of application shows some increase in fluorescence within the bundle sheath and less fluorescence in the mesophyll of these veins. Note that the small vein (LV2) shows an increase in fluorochrome accumulation within the vascular parenchyma and little in the phloem. **C.** At 3cm from the point of application, an increase in patchiness of the fluorochrome within the vascular parenchyma and intense fluorescence within the adjacent cells (MES & BS) can be seen. **D.** About 5cm from the point of application the leaves show reduced 5,6-CF fluorescence within the vascular parenchyma of small veins (LV1 & 2) but increase in fluorescence within the mesophyll associated with the small vein (LV2) and that of the intermediate vein (LV3).

LV= longitudinal vein; XV= cross vein; BS= bundle sheath; VP= vascular parenchyma; MES= mesophyll; P= phloem. (A-D) Bars = 20µm

cells. Note that there is no fluorescence within the mesophyll cells associated with this intermediate vein (LV3).

At about 2cm from the point of application (Fig 3.4B), 5,6-CF transport was observed within all veins. The small longitudinal vein (LV1) shows some evidence of 5,6-CF unloading as the fluorochrome is observed in many of the bundle sheath cells and within the mesophyll cells associated with this vein (right). Some evidence of vein unloading was also observed within the other small vein (LV2). Note that this vein shows the 5,6-CF associated fluorescence mostly within the vascular parenchyma rather than within the phloem. Intense 5,6-CF fluorescence was observed within the phloem, vascular parenchyma, and the bundle sheath of the intermediate vein.

Approximately 3cm from the point of application (Fig 3.4C) most of the longitudinal veins show patchy or discontinuous 5,6-CF fluorescence within the vascular parenchyma, which is possibly due to unloading into the adjacent cells. Increase in 5,6-CF-associated fluorescence was observed within the bundle sheath and mesophyll cells of the small longitudinal vein (LV1). In the other small vein (LV2) fluorescence were observed especially within the bundle sheath. Within the intermediate vein (LV3) 5,6-CF fluorescence was observed in all the cells associated with this vein including the mesophyll.

Approximately 5cm from the point of fluorochrome application (Fig. 3.4D), less intense 5,6-CF-associated fluorescence was observed within the vascular parenchyma cells and the bundle sheath cells, and especially within the small longitudinal veins (LV1 & 2). More intense fluorescence were seen within the mesophyll cells associated with small longitudinal vein (LV2) and intense fluorescence was also observed within the mesophyll cells associated with the intermediate vein (LV3) and thus providing the evidence of 5,6-CF unloading by these veins.

In contrast to the leaf tissue exposed to ambient carbon dioxide (Fig 3.3), leaves of plants which were exposed to elevated carbon dioxide (Fig 3.4) show more intense 5,6-CF fluorescence. A leaf tissue exposed to ambient carbon dioxide (Fig 3.3A) shows 5,6-CF associated fluorescence within the vascular parenchyma and the phloem and little in the other cells. Some was visible within the bundle sheath (far right) and the mesophyll (far left). Only in Fig 3.3C (2cm from the application point) that the leaf tissue exposed to ambient carbon dioxide show 5,6-CF associated fluorescence in all the cells. In leaf tissues from attached leaves of plants exposed to ambient carbon dioxide (Fig 3.3), the fluorochrome was transported 2cm for 3h and in leaf tissues exposed to elevated carbon dioxide (Fig 3.4) the fluorochrome traveled 5cm within the 3h experimental period.

Results obtained for the attached sink leaf material exposed to ambient (Fig 3.3) and elevated carbon dioxide (Fig. 3.4) concentrations were essentially similar, in that they both showed a typical offloading sequence towards the tip of the leaf. Furthermore the vascular parenchyma of both treatments showed evidence of discontinuous or "patchy" fluorochrome localization along the single longitudinal vein, particularly near the junction of the cross veins. As one continues along a single longitudinal vein, the fluorochrome appeared to be more intensely deposited within the vascular parenchyma and the bundle sheath cells suggesting unloading via the sieve tubes.

3.2.3 Visualization of the fluorochrome within source leaves

5,6-CFDA was introduced into the symplast of source leaves maintained at ambient and elevated carbon dioxide concentrations and illuminated at 200μm^{-2} sec $^{-1}$. Each leaf was observed 3h after the fluorochrome application and the results obtained were similar.

Fig. 3.5 (A-D) is typical of the results obtained from the leaf tissues taken from plants grown under ambient carbon dioxide concentrations. The images show a typical loading sequence within a source leaf. Longitudinal basipetal transport was observed from the point of fluorochrome application. The fluorescent front was observed approximately 3cm away from the point of 5,6-CFDA application at the end of this experiment, and on the others as well. Fig. 3.5A is at the approximate point of application and Fig. 3.5D is at approximately 2cm away from the point of application.

Fig. 3.5A which was taken at the approximate point of application of 5,6-CFDA, shows bright 5,6-CF-associated fluorescence in the mesophyll cells between the small intermediate vein (LV2) and the other vein (LV3). Some bundle sheath and most of the vascular parenchyma cells visible in this vein, also show some 5,6-CF fluorescence. A little, but bright fluorescence was observed within the phloem of the small longitudinal vein (LV3). Lateral transfer of the fluorochrome was observed via the cross vein connecting to the small longitudinal vein (LV1).

Approximately 1cm from the point of 5,6-CFDA application (Fig 3.5B), bright 5,6-CF fluorescence was observed within many of the bundle sheath cells associated with the longitudinal veins captured in this image. The first two upper longitudinal veins are small veins (LV1 & LV2) and the bottom one is an intermediate vein (LV3). Lateral transfer of the fluorochrome was also observed via the cross vein from one longitudinal vein to the other. The small longitudinal vein (LV1) and the small vein (LV2) showed some increases in fluorochrome accumulation at the vascular parenchyma and the phloem. There was absolutely no 5,6-CF-associated fluorescence observed within the mesophyll associated with these longitudinal veins.

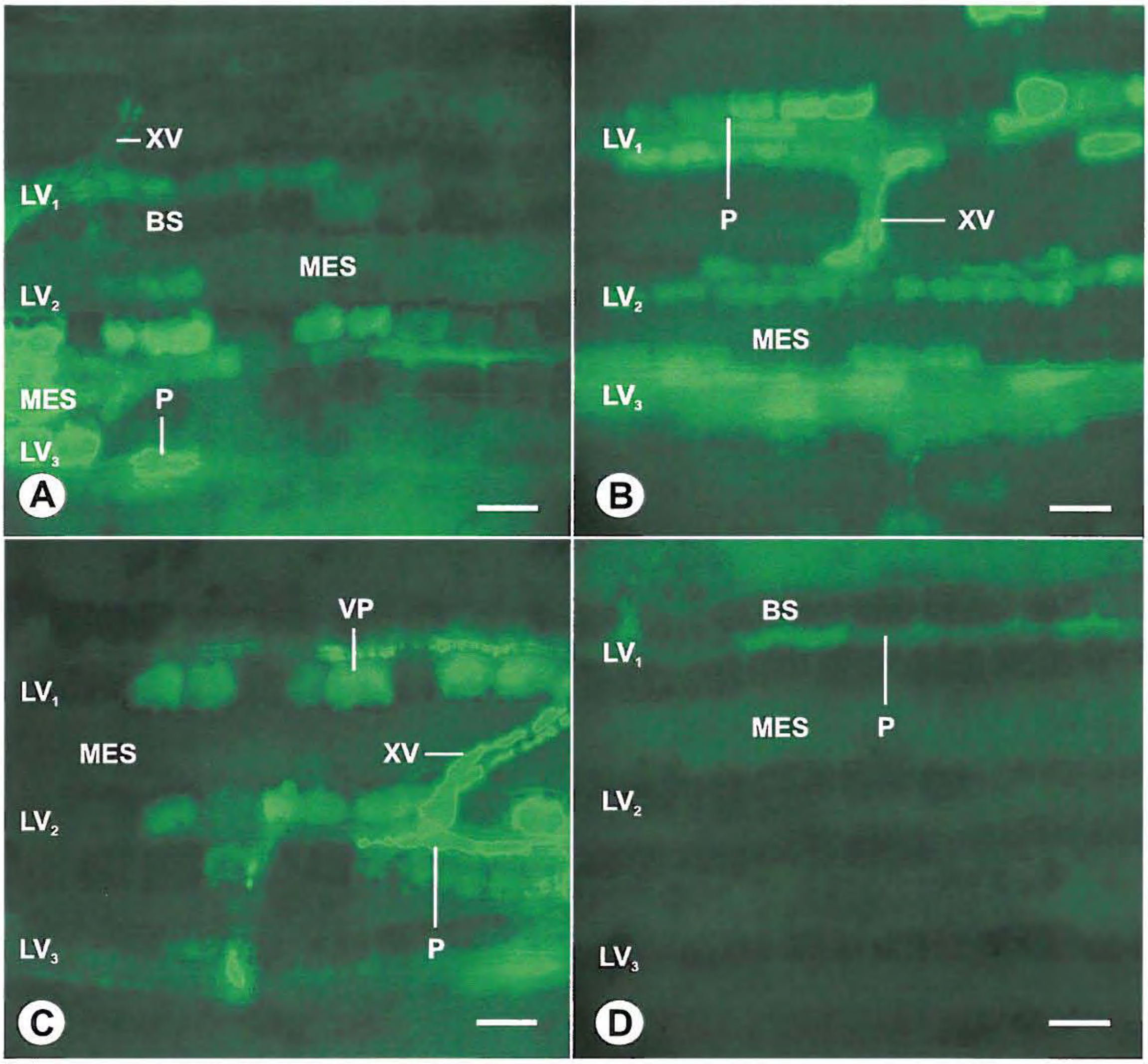
XV
LV1
BS
MES
LV2
MES
P
LV3
A
LV1
P
XV
LV2
MES
LV3
B
VP
LV1
MES
XV
LV2
LV3
P
C
BS
LV1
MES
P
LV2
LV3
D

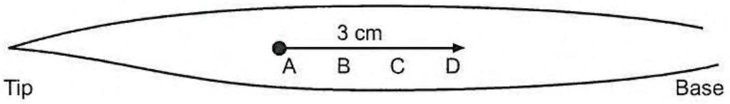
3 cm
A
B
C
D
Tip
Base

Fig 3.5: Images taken from a 30cm long source leaf, from a plant exposed to ambient CO_2 after 3h of 5,6-CFDA uptake. Note that Fig 3.5A is the closest and Fig 3.5D is the furthest from the point of 5,6-CFDA application. The fluorochrome was applied at about 15cm from the leaf base. **A.** shows the approximate point of application showing some aspects of 5,6-CF distribution within the mesophyll, bundle sheath, and vascular parenchyma associated with intermediate longitudinal vein (LV3) and with small longitudinal vein (LV2). Note 5,6-CF fluorescence within the phloem in LV3, and little fluorescence within the cross vein. **B.** At approximately 1cm from the point of intermediate vein application, bright 5,6-CF fluorescence is mostly within the bundle sheath in the longitudinal veins (LV1, 2 & 3). Note the increases in 5,6-CF accumulation at the vascular parenchyma and the phloem (LV1 & LV3). **C.** At 2cm from the point of application bright 5,6-CF fluorescence was visible in the vascular parenchyma and the phloem, with few of the bundle sheath cells showing 5,6-CF fluorescence (see, LV1 & 2). The cross veins also show 5,6-CF transport. **D.** Note 5,6-CF fluorescence shown only at the vascular parenchyma and the phloem within the small longitudinal vein (LV1).

LV= longitudinal vein; XV= cross vein; BS= bundle sheath; VP= vascular parenchyma; MES= mesophyll; P= phloem. (A-D) Bars = 20µm

Approximately 2cm from the point of 5,6-CFDA application (Fig 3.5 C), the bundle sheath showed less 5,6-fluorescence, and much more intense fluorescence was observed in the vascular parenchyma (see, LV1) and the phloem (see, LV2). The three longitudinal veins visible in this image shows interconnections by the cross veins. Intense 5,6-CF fluorescence was observed within the cross veins and thus lateral transfer of 5,6-CF between the two small longitudinal veins, (LV1 and 2). Note that there was absolutely no 5,6-CF-associated fluorescence observed within the mesophyll of all the longitudinal veins.

Less fluorescence was observed within the bundle sheath of the longitudinal veins except for one small longitudinal vein (LV1) approximately 3cm from the point of 5,6-CFDA application (Fig 3.5D). No 5,6-CF fluorescence was observed within the mesophyll of the longitudinal veins captured. Of interest is the location of the 5,6-CF fluorescence observed within the small vein (LV1). Although not brightly fluorescing, the fluorochrome was observed only at the vascular parenchyma and the phloem in this longitudinal vein (LV1).

Fig 3.6 (A-D) is an example of the results obtained from one of the eight experiments of uptake from leaves of plants exposed to elevated CO_2. The images demonstrate evidence of a typical loading sequence within a source leaf, showing longitudinal basipetal transport of 5,6-CF after the application of 5,6-CFDA. The fluorescence front was observed approximately 5cm from the point of application of 5,6-CFDA. Fig. 3.6A shows the region of application of 5,6-CFDA and Fig. 3.6D was taken approximately 5cm from the point of application.

Near to the application site (Fig 3.6A) intense 5,6-CF-associated fluorescence was visible in the vascular parenchyma of both small longitudinal veins (LV1 & LV2), whilst less intense fluorescence was associated with the phloem. The fluorescence was less intense in the bundle sheath cells within the upper longitudinal vein (LV1) and also within the mesophyll cells surrounding these veins. Some 5,6-CF-associated fluorescence was observed in the bundle sheath of the longitudinal vein (LV2). 5,6-CF associated fluorescence seen in the interconnecting cross vein shows strong fluorescence at the junction of the cross vein and the longitudinal vein.

Fig 3.6B, which was taken approximately 3cm from the point of 5,6-CFDA application, shows intense fluorescence within the vascular parenchyma in the small vein (LV1). Little if any fluorescence was associated with mesophyll cells, suggesting a strong longitudinal transport capacity within the source (transport) veins. Increases in accumulation of 5,6-CF were observed within the phloem. 5,6-CF-associated fluorescence were observed within the other vein (LV2) but seemed more likely to be spreading towards the walls of these cells as it is perhaps being loaded to the adjacent cells.

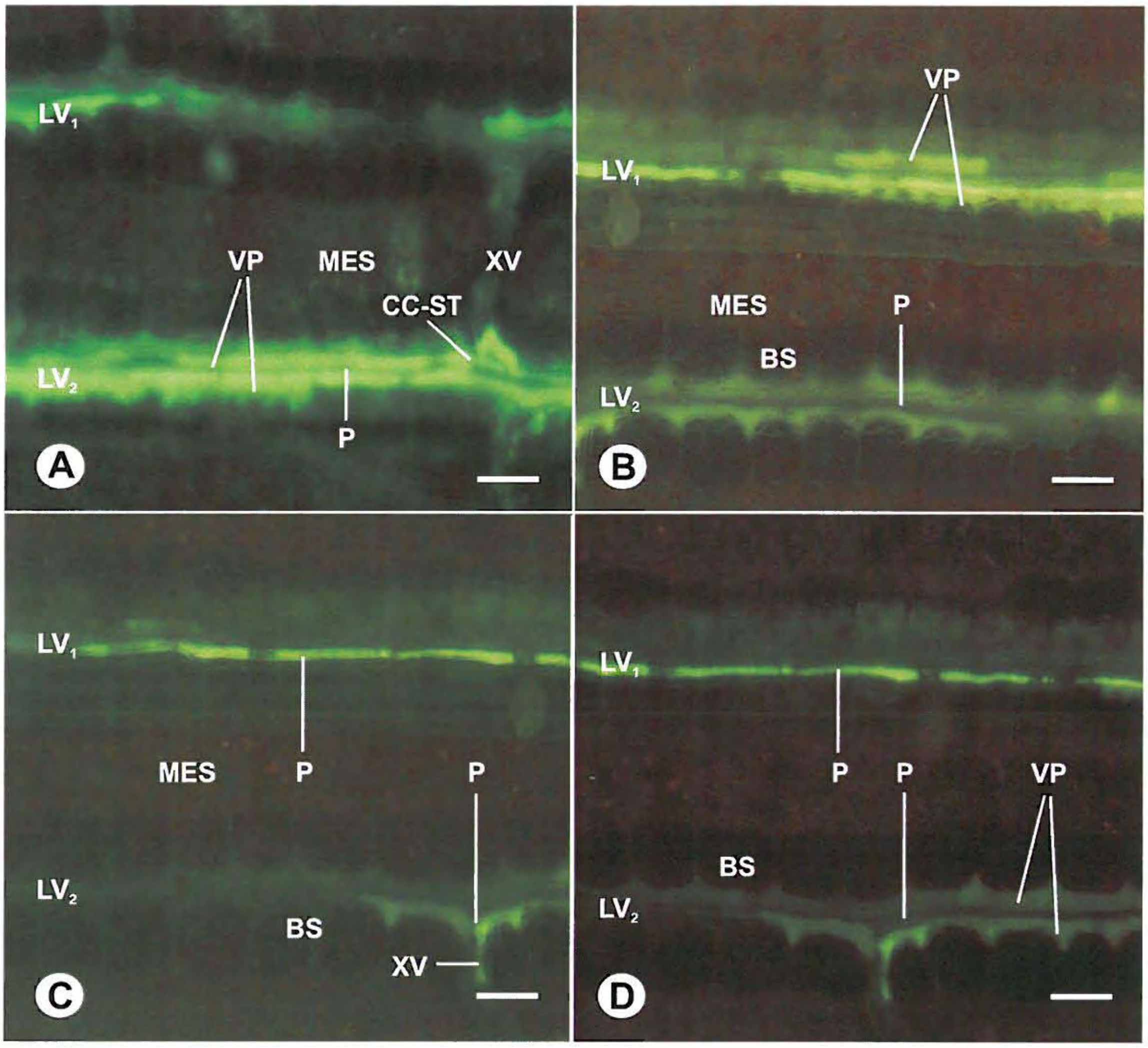
LV1
VP
MES
XV
CC-ST
LV2
P
A
VP
LV1
MES
P
BS
LV2
B
LV1
MES
P
P
LV2
BS
XV
C
LV1
P
P
VP
BS
LV2
D

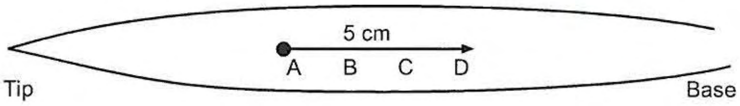
5 cm
A
B
C
D
Tip
Base

Fig 3.6: Shows images taken from a 30cm source leaf taken from a plant grown under elevated CO_2 3h after flap feeding with 5,6-CFDA. As recorded for previous plates, Fig 3.6A is closest to and Fig 3.6B is furthest from the application point. The fluorochrome was applied about 15cm from the base of the leaf. **A.** shows the region of application of 5,6-CFDA, and intense fluorescence associated with the vascular parenchyma of longitudinal veins (LV1 & LV2). Less fluorescence associated with the phloem can be seen. Note that there is less 5,6-CF fluorescence within the bundle sheath (LV1), and mesophyll cells associated with longitudinal veins (LV1 & LV2). The cross vein shows some evidence of 5,6-CF transport. Note the intense 5,6-CF fluorescing at the junction of the cross vein and what is interpreted as the companion cell-sieve tube complex. **B.** image taken at approximately 3cm from the point of application, shows 5,6-CF within the vascular parenchyma of longitudinal veins (LV1 & SV2) and the phloem. The lower longitudinal vein (LV2) shows 5,6-CF fluorescence within the bundle sheath and little 5,6-CF within the phloem. **C.** At 5cm from the point of application, fluorescence is associated with the phloem (LV2). Note that 5,6-CF is evident within the vascular parenchyma and the phloem at the junction of the cross vein. **D.** Shows 5,6-CF fluorescence within the (LV2) and some fluorescence at the junction of the cross vein, perhaps within the phloem.

LV= longitudinal vein; XV= cross vein; BS= bundle sheath; VP= vascular parenchyma; MES= mesophyll; P= phloem; CC-ST= companion cell-sieve tube. (A-D) Bars = 20µm

Approximately 5cm away from the point of application (Fig 3.6C), 5,6-CF-associated fluorescence was still observed within the phloem, (LV1 & 2). Less fluorescence was observed within the vascular parenchyma and no fluorescence was observed within the mesophyll associated with the two longitudinal veins. Little if any transport was observed within the bundle sheath (LV2). The cross vein observed emerging from the lower side of the bottom longitudinal vein (LV2) showed 5,6-CF transport from one vein to the other.

Fig 3.6D, which was taken a few mm away from Fig 3.6C, showed 5,6-CF-associated fluorescence mostly within the phloem in both longitudinal veins (LV1 & LV2). Longitudinal vein (LV2) also showed the fluorescence associated with 5,6-CF at the vascular parenchyma and little evidence of 5,6-CF fluorescence was observed within the bundle sheath in this case.

The results shown in Fig 3.5 (ambient CO_2) and 3.6 (elevated CO_2) were similar in that they both showed a typical loading sequence within a source leaf. Intense fluorescence was observed in leaves from plants which were exposed to elevated CO_2 than those at ambient CO_2.The difference was that at ambient CO_2 the fluorochrome traveled 3cm for 3h while at elevated CO_2 it traveled 5cm for 3h and provides evidence for increased phloem transport at elevated CO_2, possibly due to higher photosynthetic rates.

3.2.4 Visualization of 5.6-CF transport in the cross vein and lateral transfer in sink and source leaves

The images shown in Fig 3.3 to 3.6 show that 5,6-CF was taken up by parenchymatous elements, including the sieve tubes after application of 5,6-CFDA to lightly-abraded leaf surfaces. They also clearly show the pattern of 5,6-CF distribution within the cross and the longitudinal veins in *Zea mays*.

Fig 3.7 shows experiments in which the uptake and transport of 5,6-CF is shown at higher magnification. Fig.3.7A and B show sink leaf, and Fig 3.7C and D source leaf. In Fig 3.7A, 5,6-CF-associated fluorescence was observed possibly within the bundle sheath of the cross vein and within all the cells of the small longitudinal veins (LV1) as well as in an intermediate vein (LV2). The cross vein emerging from the small longitudinal vein (LV2), showed intense 5,6-CF. At the junction of the cross vein, fluorescence was intense especially within the vascular parenchyma of LV1. Some fluorescence was observed within the mesophyll cells and is taken as evidence of unloading.

In Fig 3.7B, strong 5,6-CF-associated fluorescence was observed within the three longitudinal veins shown here, within two small veins (LV1 &2) and the intermediate vein (LV3), as well as within the interconnecting cross veins. The cross veins show bright 5,6-CF fluorescence within the bundle sheath and less fluorescence in the phloem. At the junction of the cross vein, the vascular parenchyma of the small longitudinal vein (LV2) clearly shows lateral transfer of

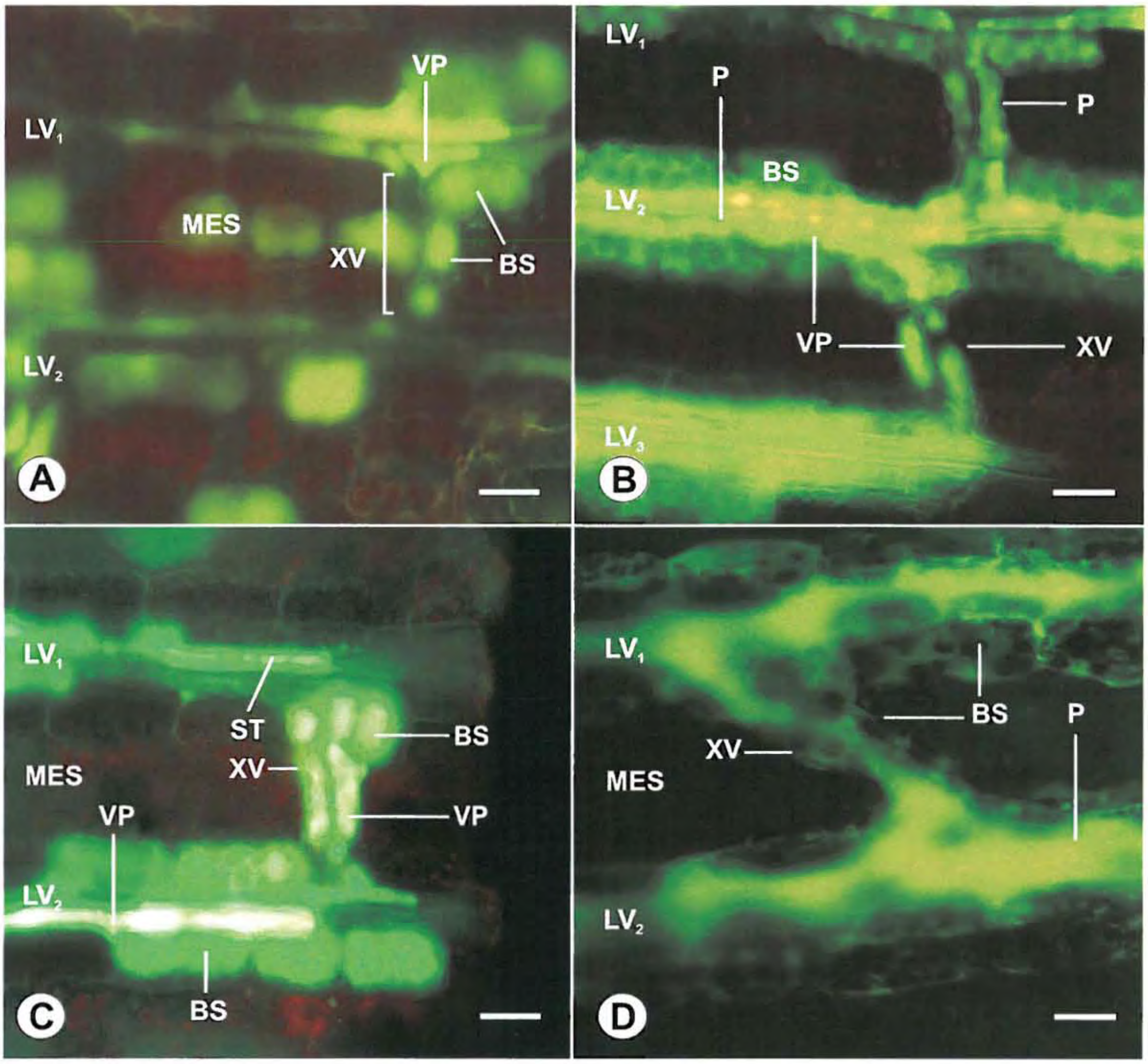
A
LV1
VP
MES
XV
BS
BS
LV2
B
LV1
P
P
BS
LV2
VP
XV
LV3
C
LV1
ST
BS
XV
MES
VP
VP
LV2
BS
D
LV1
BS
BS
P
XV
MES
LV2

Fig 3.7: shows fluorochrome localization at higher magnification, from a leaf tissue 3h after 5,6-CFDA application and illustrates lateral transport via the cross vein. Figs 3.7A & B from sink and Fig 3.7C & D source leaf material. A shows the distribution of 5,6-CF within the mesophyll, vascular parenchyma and the bundle sheath cells of both the cross and the longitudinal veins. Note 5,6-CF transfer into the cross vein via the vascular parenchyma. B shows 5,6-CF transport via the three longitudinal veins and lateral transport via the two interconnecting cross veins. Note the brightly fluorescing 5,6-CF within the vascular parenchyma and the phloem of the small longitudinal bundles (LV2) also evident within the sieve tube at the junction of the cross vein. C shows bright 5,6-CF fluorescence within the cross vein and also within the longitudinal veins. The cross vein shows intense 5,6-CF fluorescence within the vascular parenchyma and also possibly in the phloem. 5,6-CF is shown within the small longitudinal veins (LV1 & 2) and possibly within the phloem in the other small longitudinal vein (LV1). D shows a source leaf showing lateral transfer of 5,6-CF via the cross vein and also showing longitudinal transport. Although not easily identifiable, all the cells of this cross vein show 5,6-CF fluorescence. Note the highlighted cytoplasmic strands within the bundle sheath, suggesting that the cytosol, and not the chloroplasts contain the fluorescence.

LV= longitudinal vein; XV= cross vein; BS= bundle sheath; VP= vascular parenchyma; MES= mesophyll; P= phloem. (A-D) Bars = 10µm

5,6-CF via the vascular parenchyma probably into the phloem of the cross vein to the intermediate vein. Bright fluorescence was observed within the phloem in the small longitudinal vein (LV2). Chloroplasts were outlined (fluorescence in the cytosol surrounding the chloroplasts) in the bundle sheath of both the cross and the longitudinal veins.

In source leaves allowed to transport 5,6-CF for 3h (Fig 3.7C), fluorescence was observed within the bundle sheath cells of the small longitudinal veins (LV1 & 2) and the vascular parenchyma of the interconnecting cross vein. Chloroplasts are outlined by 5,6-CF, which is in the surrounding cytosol (see, LV2). Strong fluorescence was observed within the vascular parenchyma and the phloem of the longitudinal veins. Within the upper longitudinal vein, strong fluorescence was observed, in the vascular parenchyma and in the sieve tubes of this vein.

In Fig. 3.7D shows intense fluorescence within the bundle sheath of both the cross and the longitudinal veins. Note the outlined chloroplasts and the cytoplasmic strands within the bundle sheath of these veins, which contains 5,6-CF. The clear areas surrounding the cytoplasmic strands are most likely non-cytosolic part and possibly vacuoles suggesting that 5,6-CF did not cross the tonoplast into the vacuole. Fluorescence associated with 5,6-CF occurred within the sieve tubes of the cross vein as well as within the vascular parenchyma and as well as in the phloem of the longitudinal veins.

The illustration shown here suggest that the vascular parenchyma seemed to be involved in the lateral transfer of the fluorochrome, as these cells showed intense fluorescence especially at the junction of the cross vein. Higher magnification images were also helpful in outlining the contents of the cells, for example chloroplasts and cytoplasmic strands within the vascular bundles.

3.2.5 Visualization of 5,6-CF within the sieve tubes in sink and source leaves

The images shown in Fig 3.7 (A-D) clearly demonstrate the involvement of the cross vein in lateral transfer of 5,6-CF between longitudinal veins. However, it is not clear from the images if 5,6-CF reached the sieve tubes or not, as the available microscopic techniques were not really powerful enough to resolve this, or to provide answers to the question. In order to positively identify the cells that were associated with 5,6-CF, double staining with aniline blue was attempted, to localize the phloem (aniline blue used to visualize the callose associated with sieve plates) after application of 5,6-CFDA uptake and transport.

Leaf strips which had been fed with 5,6-CFDA for 3h, were scraped and then stained with aniline blue, allowed to stand for 10min to develop the callose response to allow identification of the cells associated with the phloem via callose deposits and to allow the location of 5,6-CF transport within these cells. Fig 3.8A and B show details of a sink leaf and Fig 3.8C, D and E details of a source leaf.

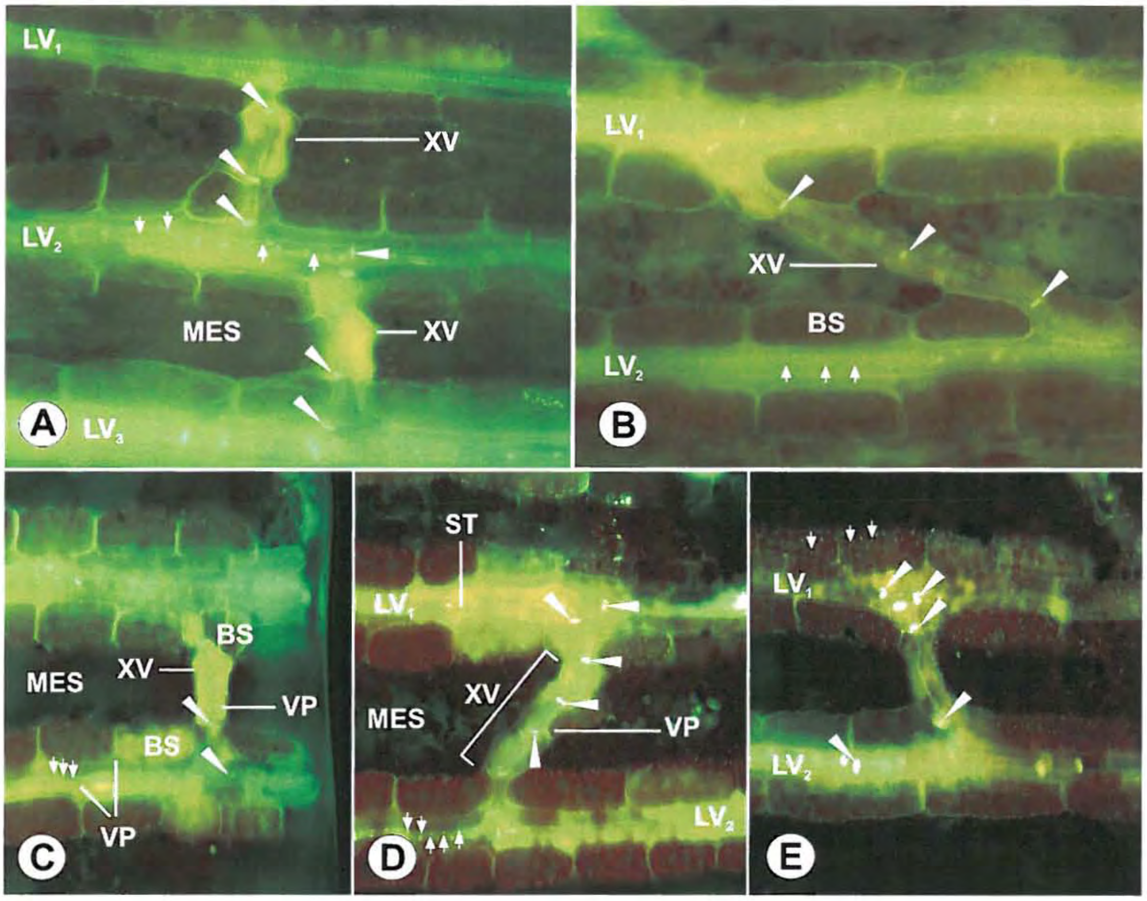
LV1
XV
LV2
MES
XV
A
LV3
LV1
XV
BS
LV2
B
BS
MES
XV
VP
BS
VP
C
ST
LV1
MES
XV
VP
LV2
D
LV1
LV2
E

Fig 3.8: shows details taken from a leaf tissue 3h after 5,6-CF application and after 10min counterstain in aniline blue, showing 5,6-CF transport within the sieve tube of the cross vein and that of the longitudinal bundles. Fig 3.8A & B from sink leaf tissue and Fig 3.8C, D and E from source leaf tissue. **A** shows three longitudinal veins and their associated cross veins. Bright callose deposits (arrowheads) occur on sieve plates in both the cross and the longitudinal veins. Each cross vein is made up of three sieve tube members which contain 5,6-CF. Note 5,6-CF within the longitudinal veins. Punctate deposits are associated with plasmodesma and were observed within the intermediate and the small longitudinal veins. **B** sink leaf, showing longitudinal veins interconnected by a cross vein. Callose deposits occur on sieve plates (arrowheads) within all the veins. One of the three sieve tube members in the cross vein is loaded with 5,6-CF as are the sieve tubes in the longitudinal vein. **C** source leaf, showing sieve plates highlighted by callose in the cross and the longitudinal veins (arrowheads). The cross vein shows two sieve tube members with 5,6-CF. The longitudinal veins show 5,6-CF fluorescence within the bundle sheath cells, the vascular parenchyma and the phloem. Punctate callose deposits within the longitudinal vein are associated with pore plasmodesmatal units and plasmodesmatal aggregates (short arrows). **D** source leaf, showing distribution of 5,6-CF within three of the five sieve tube members of the cross vein and within the sieve tube of the small longitudinal veins. Sieve tubes were identifiable as bright callose deposits at the sieve plate (arrowheads) were seen. Punctate callose deposits at the phloem are plasmodesma (short arrows). **E** source leaf tissue, showing bright callose deposits associated with sieve plates within the cross vein and the longitudinal veins (arrowheads). All the sieve tube members observed show 5,6-CF-associated fluorescence.

LV= longitudinal vein; XV= cross vein; BS= bundle sheath; VP= vascular parenchyma; MES= mesophyll; arrowheads= sieve plates; short arrows= pore plasmodesma units and plasmodesma. (A-D) Bars = 10µm

In Fig 3.8A, lateral transport of 5,6-CF was observed via the cross vein interconnecting two small (LV1 & LV2) and one intermediate bundle (LV3). In both cross veins, bright fluorescence associated with 5,6-CF was clearly observed within the vascular parenchyma cells. Although not fluorescing brightly, 5,6-CF appeared to be localized within the sieve tubes of the two cross veins, which was confirmed by the presence of callosed sieve plates (arrowheads). The cross veins shown here contain three sieve tube members, joined end to end by sieve plates. Callose deposits associated with sieve plate pores (arrowheads) were also observed within the longitudinal bundle (LV2). Although not fluorescing as brightly, punctate deposits, associated with plasmodesmatal aggregates and pore plasmodesmatal units are visible between the vascular parenchyma and companion cell-sieve tube complex within the small longitudinal vein (LV2) as well as in the intermediate longitudinal vein (LV3, short arrows).

In Fig 3.8B, callose deposits were observed associated with the sieve plate pores (arrowheads) within the small longitudinal bundles (LV1 &LV2) and within the cross vein interconnecting the two. The callose punctate deposits (short arrows) observed within the small longitudinal vein (LV1) and the intermediate vein (LV2) are associated with plasmodesmatal aggregates and pore plasmodesmatal units at the vascular parenchyma and the phloem (located by short arrows). Note that the cross vein is made up of three sieve tube members connected end to end by sieve plates. The fluorochrome is contained within one of the three sieve tube members of the cross vein. The sieve tube of the small longitudinal vein (LV1) is identifiable via sieve plates (arrowheads), also showing 5,6-CF fluorescence at this site.

It was possible to identify the cells associated with the phloem by looking at the location of the callose deposits (Fig 3.8C). The sieve tube within the cross vein was identified because of callose deposits at the sieve plates (arrowheads). Although not always apparently entire, bundle sheath cells were observed surrounding the cross veins. This made it difficult to see other cells including the phloem. Note 5,6-CF associated fluorescence observed within the visible sieve tube member of the cross vein. The sieve tube of the small longitudinal vein (LV2) was also identifiable through callose associated fluorescing aggregates between the companion cells and the sieve tube (short arrows). These aggregates correspond to numerous pore plasmodesmatal units at this interface. Plasmodesmatal aggregates were also observed via callose deposits at the vascular parenchyma-bundle sheath interface (short arrows). 5,6-CF-associated fluorescence was seen within the phloem, including the sieve tubes as well as within adjacent vascular parenchyma cells in the longitudinal veins. It is therefore quiet likely that 5,6-CF reached the sieve tubes via a symplasmic pathway.

In Fig 3.8D, the sieve tubes can be identified by the presence of callose on the sieve plates (arrowheads) in the cross vein. Note that the sieve tube of the cross vein is composed of five sieve tube members connected end to end via the sieve plates. Lateral transfer via the cross vein occurred in this instance. The sieve tube members of the longitudinal bundles were also identifiable via the sieve plates (arrowheads, LV1). Fluorescing aggregates associated with callose deposits were observed between the vascular parenchyma and the bundle sheath (short arrows, LV2). Also note the observed plasmodesma at the phloem site (short arrows, LV2). 5,6-CF associated fluorescence was highlighted within the vascular parenchyma and the sieve tube in both veins. It was possible to visualize the connection of the sieve tube of the cross vein to that of the longitudinal vein (LV2) via callose deposits.

In Fig 3.8E, strong fluorescence associated with callose deposits were observed on the sieve plates (arrowheads) within the longitudinal veins as well as within the cross vein. Two sieve tube members were visible within the cross vein. The other punctate deposits (short arrows) within the other cells are associated with plasmodesma.

Aniline blue was used as a counterstain and applied after 5,6-CF transport had occurred, allowed positive identification of the phloem components to be made. Although the technique was not easy, it has clearly shown that 5,6-CF was taken up and was translocated via the sieve tubes.

3.2.6 Apoplasmic retrieval from the xylem to the phloem

While the figures shown in 3.8(A-E) illustrate that 5,6-CF was taken up by the phloem, there are still questions about how and where this uptake can take place. One of the questions posed was, could 5,6-CF be retrieved from the apoplast? If it was, what was the route which was followed? Where would 5,6-CF first appear after cleavage? To answer the questions required that experiments using cut leaves with their cut ends dipped in 5,6-CFDA would be allowed to take up 5,6-CFDA in the transpiration stream. Localization of 5,6-CF was studied after several hours.

After 120 and 180 min, the leaves were examined for 5,6-CF distribution and then cut into silicone oil as detailed in the materials and methods or, the cut end leaves were immediately transferred to a weak 3-kD Texas Red dextran solution, which was taken up in the transpiration stream. The leaves were quickly examined to localize the Texas red front. Sections were cut and examined using the relevant fluorescence filter cubes and the images using SIS Software.

Fig 3.9A shows part of a transverse section of a sink leaf with a large (transporting) and a small (unloading) vein connected via a transverse vein after 3h of 5,6-CF transport and 1h of chasing with Texas Red. The large vein shows no 5,6-CF fluorescence and all the cells associated with the xylem are stained with Texas Red. In contrast, within the small bundle, 5,6-CF is distributed throughout the phloem, the bundle sheath and the mesophyll cells. The xylem vessels are stained with Texas red. The connecting cross vein shows some evidence of 5,6-CF transport.

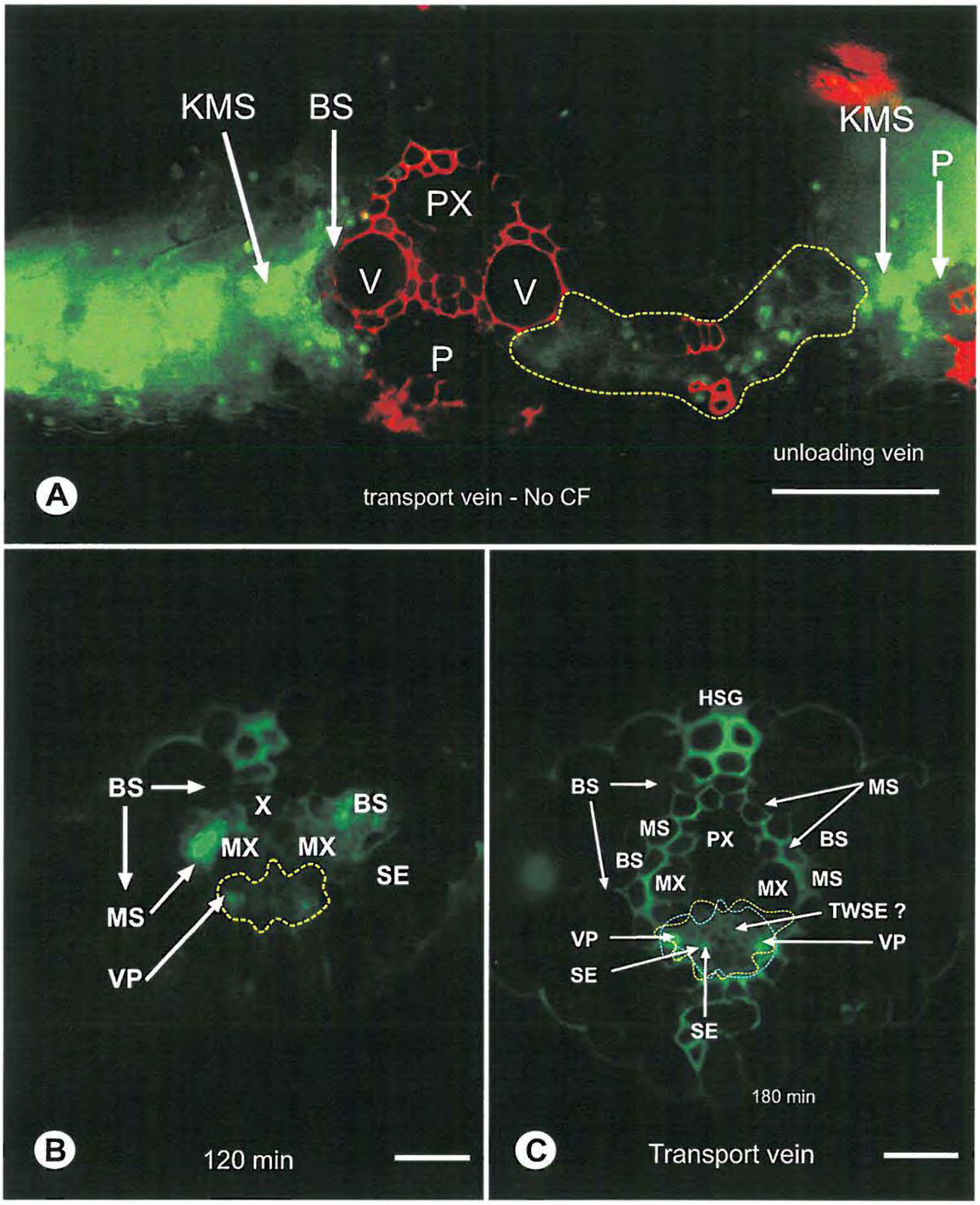
KMS
BS
PX
V
V
P
KMS
P
unloading vein
A
transport vein - No CF
BS
X
BS
MX
MX
SE
MS
VP
B
120 min
HSG
BS
MS
MS
PX
BS
BS
MX
MX
MS
TWSE ?
VP
VP
SE
SE
180 min
C
Transport vein

Fig 3.9: Transverse sections cut from a freshly prepared maize leaf showing the vascular bundles involved in 5,6-CF transport and translocation pathway of 5,6-CF within the phloem. **A.** Functional xylem elements are stained with Texas Red and 5,6-CF fluorescence was observed within the large vein. Intense 5,6-CF fluorescence was seen in all cells of the small vein except for the xylem vessels, which are stained with Texas Red. **B.** image taken 120 min after 5,6-CFDA application showing 5,6-CF fluorescence associated mostly with the xylem parenchyma and the bundle sheath. **C.** After 180 min 5,6-CFDA application showing 5,6-CF within the phloem parenchyma and possibly associated with thin-walled sieve tubes. Very faint fluorescence was located near to the presumed location of the thick-walled sieve tubes.

BS= bundle sheath; MES= mesophyll; VP= vascular parenchyma; XV= cross vein; MX= metaxylem, PX= protoxylem; SE= thin-walled sieve tube; TWSE= thick-walled sieve tube. Dotted further= zone of the phloem (A) Bar = 100μm, (C & D) Bars= 50μm

Fig 3.9B shows a transverse sections of a transporting vein after 120 min of 5,6-CF application. Less 5,6-CF fluorescence was observed within the vascular parenchyma adjacent to the xylem vessels and probably within the phloem parenchyma. Intense fluorescence was observed within the bundle sheath cells located near to the xylem vessel. 180min after 5,6-CFDA application (Fig 3.9C), fluorescence was observed within the phloem parenchyma possibly some thin-walled sieve tubes and there was sometimes fluorescence in the vicinity of the thick-walled sieve tubes.

CHAPTER 4: DISCUSSION

4.1 Anatomy of the leaf

The data presented in this study showed that the vascular bundle of maize leaf was typical of the monocotyledonous species and possesses well-defined phloem, consisting of large diameter sieve elements with companion cells. Contacts were always found between the sieve tube of the cross vein and that of the longitudinal veins (Fig 3.1A & B; see also Fritz *et al.* 1983). The sieve tubes of the cross veins were either connected to the thin-walled (Fig 3.1A) or to the thick-walled sieve tubes (Fig 3.1B) of the longitudinal veins (see also Fig 17 and 18 in Fritz *et al.* 1983). The xylem comprised two large metaxylem vessels and usually a single protoxylem element with an associated lacuna. In consistence with Evert *et al.* (1978) the bundle sheath was not always entire, especially in the light microscopy studies.

4.2 High CO_2 effects on transport

Sink (Fig 3.4) and source (Fig 3.6) leaf tissues exposed to elevated CO_2 showed increases in transport rates and intensities of 5,6-CF. These increases in transport rates and 5,6-CF intensities observed in the present study could be due to the pronounced increases in carbohydrate accumulation at elevated CO_2 (Apel, 1976; Cave *et al.* 1981; Preiss, 1982; Thomas and Harvey, 1983; Cure and Acock, 1986; Vu *et al.* 1989; Bowes, 1991; Lawler and Mitchell, 1991; Madsen, 1968; Stitt, 1991; Wolfe and Erickson, 1993; Conroy *et al.* 1994; Kutik *et* *al.* 1995; Pritchard *et al.* 1997). In contrast, Nafziger and Koller (1976) noted a strong inverse relationship between amounts of leaf starch and rates of photosynthesis in *Glycine max*. These authors suggested that accumulation of starch might have increased the diffusive resistance to intracellular CO_2 transport, thereby lowering photosynthesis. Furthermore, they have suggested that such excessive starch accumulation might interfere with cytoplasmic streaming, further impeding intracellular CO_2 transport.

Studies by Korner *et al.* (1995) suggested that following exposure to elevated CO_2 structural carbohydrates are increased by 47% in symplasmic loaders compared to 25% observed in apoplasmic phloem loaders. The extremely high TNC concentrations observed by symplasmic phloem loaders therefore suggested that there is a greater demand for transport capacity under elevated CO_2. This study also opened new perspectives by questioning if species are able to increase the amount of phloem terminal tissue in order to cope with this greater demand for transport capacity under elevated $CO_{2.}$

Variable results have been obtained from studies dealing with changes in the phloem area in different species exposed to elevated CO_2. St Omer and Horvath (1984) observed an increase in the vascular regions of leaves of *Layai platyglossa* exposed to elevated CO_2, which they attributed to larger vascular elements. Ho (1977) found no difference in the petioler phloem cross-sectional area of tomatoes grown in elevated CO_2. An increase in the vascular tissue cross-sectional area has also been reported for pine species (Thomas and Harvey, 1983; Conroy *et al.* 1986) however in these studies the phloem tissue was not measured separately from the xylem. Pritchard *et al.* 1997 studied the vascular anatomy of pine species at different nutrient levels and at elevated CO_2. Their studies (Pritchard *et al.*1997), demonstrated a reduction in total number of cells within the phloem and phloem cross-sectional area was also reduced at elevated CO_2. Furthermore, the phloem sieve cells of plants exposed to elevated CO_2 by low nutrient and well-watered treatments were significantly flattened compared to ambient CO_2. Lee (1981) suggested had earlier on suggested that regardless of the mechanism, a small decrease in the radius of sieve cells can cause a major decline in the capacity of phloem to transport fluid. Based on the above studies an assumption could be reached that the increases in transport rates observed under elevated CO_2 are due to a possible increase in the phloem tissue of these plants and therefore increases in transport capacity.

Hartt (1966) believes that "translocation of photosynthate is independent of the assimilation of carbon" and "for this reason sugar transport may be a phototranslocation and the initiation of translocation of sugar from the leaf may be under photocontrol". Experiments from plants exposed to same light levels but different CO_2 concentrations suggest that light intensity play an important role by only acting on photosynthesis (Heyser *et al.* 1975). From the present experiments it seems that the difference in 5,6-CF intensities and transport rates depend upon the irradiation to which the leaf is subjected. At normal photosynthetic conditions (high light conditions and higher CO_2 concentrations), the loading and the transport processes proceed more rapidly but at low CO_2 and same light conditions, it proceeds more slowly.

4.3 Implication of plasmodesmata in symplasmic loading as visualized via Aniline blue fluorescence

When maize leaf strips were treated with aniline blue, callose was observed associated with sieve plates and plasmodesma between the vascular parenchyma and the bundle sheath cells as well as between sieve tube-companion cell complex (Fig. 3.2B & C) of the longitudinal veins and also between the sieve tube and the companion cell in the cross vein (Fig 3.2A) demonstrating at least a potential for a symplasmic transport pathway. The connection of the cross vein sieve tubes to those of the longitudinal veins was identifiable either by callose deposited at the sieve plates or at the plasmodesmata (Fig 3.2A-E). Callosed-occluded plasmodesmata seen (short arrows, Fig 3.2B & C) suggest that the plasmodesmata at this location are normally gated open. The activation of the wound response due to loss of turgor pressure has resulted in the closure of the plasmodesmata by the deposition of callose (Hughes & Gunning, 1980; Lucas *et al.* 1993).

Similar to studies in *Allium cepa* (Currier and Strugger, 1955), sieve plates were found to fluoresce the most in the present study (Fig 3.2). It has been suggested that callose is found to accumulate there normally (Currier, 1957) and becomes more concentrated after wounding (Smith & McCully, 1978). Aniline blue studies in living epidermis of *Allium cepa* (Currier, 1957) suggested that increased staining occurred with time but this 10 min and 0,05% of aniline blue was found to be suitable to stain sieve plates and other areas associated with the phloem in different species.

4.4 Does Zea mays leaf blade phloem load syplasmically?

A prerequisite for symplastic transport is the presence of plasmodesmal aggregates or sites between the vascular parenchyma and the companion cell-sieve element complex. If the leaf apoplast is subdivided by cell walls, separating mesophyll cells and vascular bundles, water-soluble components can cross this barrier along a symplastic route only. This is apparently the case in maize (Evert *et al.* 1977a) and in wheat (Kuo and O'Brien, 1974) where numerous plasmodesmata perforate the cell walls between the mesophyll and bundle sheath cells. Plasmodesmal connections may, however, be rare or absent between the sieve element-companion cell and adjacent cells (Evert *et al.* 1978), suggesting loading from the apoplast by a membrane-transport process. The same argument prevails in sink leaves, where the protophloem sieve tubes were found also to be isolated symplastically from the rest of the leaf (Evert and Russin, 1993).

Although anatomical and ultrastructural studies in maize leaves have suggested that the phloem loading and unloading pathway is from the apoplast (Evert *et al.* 1978; Evert & Russin, 1993), a symplastic transport pathway must exist as the experiments reported here using membrane impermeable dyes have demonstrated the presence of 5,6-CF in the phloem. If the fluorochrome is in the phloem, then some plasmodesmal connections must exist to allow passage of the fluorochrome. Although it is well known that 5,6-CFDA is a membrane impermeant fluorochrome, it is possible that it crossed the vascular parenchyma and the companion cell-sieve element barrier, was metabolized in the companion cells and loaded via pore-plasmodesma into the sieve tubes.

Fluorescent compounds such as 5,6-carboxyfluorescence (5,6-CFDA) have been used previously for many years to demonstrate a symplasmic mode of phloem loading within plants (Turgeon and Hepler, 1989; van Kesteren *et al.* 1988; Farrar *et al.* 1992; Haupt *et al.* 2000). Applied in a diacetate form, these esters are able to cross the membrane and do not fluoresce. It is the carboxyl group present in CF that results in this molecule being less membrane permeant and more suitable as a phloem probe (Grignon *et al.* (1989), although some membrane permeant ions could be present under more acidic physiological conditions and therefore accumulate in cell vacuoles. Grignon *et al.* (1989) introduced CF into leaves of petioles of soybeans and found it to be phloem transported over long distances, without leakage to the apoplast and the transport obeyed the rules of phloem sap transport from source to sink regions. 5,6-CF remained confined within the phloem even after 4 days of application. Fig 3.7D shows cytoplasmic strands surrounded by clear areas, possibly vacuolar regions, suggesting that 5,6-CF did not cross the tonoplast into the vacuole. Furthermore the fluorochrome in Fig 3.7 (B & D) is in the cytosol sorrounding the chloroplasts. Grignon *et al.* (1989) also determined the apparent pK_a (6.3) and log K_{ow} (-1.5) of the molecule and stated that it was suited to transport in the phloem, as predicted from models of phloem transport based on pK_a and log K_{ow} of several xenobiotics (Kleier, 1988). Oparka (1991) suggested that these dyes should be treated with caution when working with as the molecule could be present as undissociated forms at percentages lower than 0.01% and would make a significant contribution to the intercellular movement of this probe (Wright and Oparka, 1996) in longer-term experiments.

Although fluorescence studies proved to be successful in demonstrating the pathway from the mesophyll cells to the sieve tubes, their data only demonstrate the presence of a symplasmic pathway, but was far from showing the occurance of symplasmic loading. In barley leaves injected with Lucifer yellow (LYCH), Farrar *et al.* (1992) noted a transport rate of approximately $3.5 \mu ms^{-1}$ or about 1.2 cmh^{-1}. In the present study 5,6-CFDA was used to trace symplasmic transport from the mesophyll to the sieve tube in sink (Fig 3.3 & 3.4) and source (Fig 3.5 & 6) leaves of maize. Transport rates of approximately 2cm in 3h for plants exposed to ambient CO_2 and 5cm in 3h at elevated CO_2 were observed. These data (1-1.2 cmh^{-1}) are then in agreement with the slow transport rates reported for Barley. However one must take into account the fact that the transport rate determined here includes the time frame needed for uptake and metabolic cleavage of 5,6-CFDA. The rate of transport could thus be very much higher, if the loading physiology was more clearly understood.

It has been suggested in literature that plasmodesmal frequency decreases along the loading route from the bundle sheath to the phloem (Evert *et al.* 1978; Ding *et al.* 1988; Botha, 1992; Botha and van Bel, 1992; Evert *et al.* 1996). Although the companion-sieve tube was found to be symplasmically isolated from the other cells, plasmodesmata frequency studies in maize (Evert *et al.* 1977a; Evert and Russin, 1993) reported a low frequency between the vascular parenchyma and the sieve tube. These plasmodesmatal frequency studies suggest a low plasmodesmal continuity at this site and therefore favouring an efficient apoplasmic loading process and in contrast an inefficient symplasmic pathway. The low plasmodesmatal frequencies observed at this site support the slow transport rates of 1.2 cmh^{-1} obtained in the present study.

The thick-walled sieve tubes in maize are argued to be well connected to the adjacent vascular parenchyma cells (Evert *et al.* 1978; Evert and Russin, 1993) suggesting a potential continuous symplasmic pathway from the mesophyll to the thick-walled sieve tube.

Based on previous microautoradigraphic studies, different bundle orders serve different functions in leaves of many species (Lush, 1976; Altus and Canny, 1982; Fritz *et al.* 1989; Evert *et al.* 1996). In all cases the small and intermediate bundles have been implicated in short distance transport and in the collection of photosynthate while larger veins are assumed to be involved with long distance transport. Results of fluorescence studies presented in Barley leaf (Haupt *et al.* 2001), suggest that phloem unloading occurred only from the major longitudinal veins. In contrast to Haupt *et al.* (2001), this study provides the solid evidence that the small veins are involved in the loading and unloading function rather than in a principally transport function, as these small veins show less fluorescence than the larger ones (showing fluorescence in all the cells) in the transport region (Fig 3.4A & B). Judged by the decline in intensity of the fluorochrome in the transport region of the smaller bundles in source leaves, it can be assumed that longitudinal transport in small bundles decreases with increasing distance from the site of loading (Fig 3.5 & 3.6). Larger veins in sink leaves show intense fluorescence in the transport region, that is before unloading occurs, therefore providing evidence for a major transport function by these veins (Fig 3.3 & 3.4). The observed results therefore support the contention that all vascular bundles in the maize leaf are functioning in loading and unloading but it is mostly the small veins that are involved in loading, and the larger ones, transport as suggested by Fritz *et al.* (1989). Transport studies in a leaf of a dicotyledonous species, *Nicotine benthamiana* demonstrated by Roberts *et al.* (1997) also showed that unloading of 5,6-CF could occur from longitudinal major veins (class 1 and 2) but the bulk of unloading occurred symplasmically from the minor (class 3) veins.

It is important to recognize the role of the numerous transverse veins in the leaf. Transverse veins have been reported to be responsible for lateral transport between longitudinal veins (Altus and Canny, 1982). Although 5,6-CFDA was introduced in a small window opened within the mesophyll, the fluorochrome did not only travel longitudinally but spread across the leaf, suggesting that assimilates loaded to the small and intermediate veins is moved across the leaf for some distances before it is transported longitudinally out of the leaf by larger bundles (Fig 3.3-3.6). Results obtained from Fig 3.7 and Fig 3.8 are also supportive of lateral transfer via the cross veins.

4.5 The role of the thin- and thick-walled sieve tubes

The presence of thin- and thick-walled sieve tubes in monocotyledonous leaves has been the subject of speculation with respect to function since Kuo and O'Brien reported their presence in 1974. It was first suggested that the thick-walled sieve tubes in wheat maybe specialized for either long distance transport, or that it could serve as a temporary storage reservoir for sugar, in excess of what can be transported by the thin-walled sieve tubes. In a microautoradiographic study in maize source leaf, Fritz *et al.* (1983) provided a strong evidence for separate roles for the thin- and thick-walled sieve tubes. ^{14}C was introduced as sucrose via the apoplast (cut leaf ends). The ^{14}C labeling experiments demonstrated that in all the bundles used, the first cells to be labeled were the vessels and with increasing time they became heavily labeled. The second most heavily labelled cells were the vascular parenchyma followed by about 35% of the thick-walled sieve tubes. In contrast less than 1% of the thin-walled sieve tubes were labeled and very few of the labeled ones were associated with the companion cells. However, it was observed that a greater proportion of thin- and thick-walled sieve tubes were labeled with increasing time. After 4-min of ^{14}C feeding, about 58% of the thick-walled sieve tubes were labeled and 45% of the thin-walled sieve tubes were labeled and after 6-8-min, 80 thin-walled sieve tubes were labeled. These studies clearly demonstrated that the vascular parenchyma abutting the vessels act as intermediary cells, first by retrieving the solutes from the vessels, and then transferring the solutes to the thick-walled sieve tubes then to the thin-walled sieve tubes as few of these were found to be associated with the companion cells. The results observed by these authors confirm the plasmodesmal frequency studies in *Zea mays* (Evert *et al.* 1978) inasmuch as many symplasmic connections were demonstrated between the vascular parenchyma and the thick-walled sieve tubes and therefore a symplasmic pathway is possible at this interface.

Using $^{14}CO_2$, Fritz *et al.* 1983 demonstrated that with increasing time, the most heavily labeled of the two sieve tubes was the thin-walled sieve tube. At 5 min chase 85% of the thin-walled sieve tubes were labeled compared with 38% of the thick-walled and after 5-min chase all of the thin-walled sieve tubes were labeled with about 90% labeled thick-walled sieve tubes. Clearly, this study demonstrated that the thin-walled sieve tubes are primarily involved with uptake while the thick-walled sieve tubes may function predominantly with retrieval of solutes from the xylem. The observations made by these authors are consistent with those of Matsiliza & Botha (2002) on preferential studies by an aphid *Stobion yakini* feeding on Barley leaves where 85% of the aphid stylet tracks terminated at the thin-walled sieve tube suggesting that perhaps it is the most functional of the two sieve tubes.

Microautoradiographic studies (Evert, 1986; Fritz *et al.* 1983; Fritz *et al.* 1989) showed contacts between the sieve tube of the cross vein and those of the longitudinal bundles. In the present study, aniline blue was used as a counter-stain after application and transport of 5,6-CF. The phloem components that are involved in longitudinal and lateral transport of 5,6-CF in both sink and source leaves could thus be clearly resolved (Fig 3.8). Due to their association with the companion cell, the sieve tube of the cross veins were usually regarded as the thin-walled sieve tube (Evert *et al.* 1978). Association of these sieve tubes with 5,6-CF fluorescence has provided direct evidence of symplasmic transport within the thin-walled sieve tube of the cross vein, and by inference, suggests that the thin-walled sieve tube of the cross vein must or should be connected to the thin-walled sieve tube of the joined longitudinal vein.

4.6 Apoplastic retrieval from the xylem to the phloem

Although the results using 5,6-CF as a symplasmic marker were successful, it cannot be denied that this fluorochrome may have entered either the thin-walled sieve tube or the companion cell-sieve tube in an undissociated form. However cleavage sites could be clearly demonstrated in uptake studies. A study of the vascular bundles in maize leaf (Evert *et al.* 1978) suggested that entry of solutes into the cell wall from the lumina of the vessels maybe facilitated by the swollen, loosely fibrillar nature of the primary walls of the vascular parenchyma cells where they abut portions of vessels lacking secondary thickening. Kuo *et al.* (1972) reported that ferric salts entered the cell walls in the wheat only at sites of such primary walls. This was supported by Prussian blue experiments in maize leaf (Evert *et al.* 1985) suggesting that the hydrolysed walls between the tracheary element and the xylem vascular parenchyma is porous and may present an access point for apoplasmic or symplasmic transfer of solutes. These authors clearly demonstrated the role of the apoplast in the loading of sieve tubes with ^{14}C-labeled sucrose taken up initially by vessels. Uptake experiments (Fig 3.9B and C) demonstrated that 5,6-CF appeared first in the xylem parenchyma adjacent to the large metaxylem and were possibly transferred radially via the bundle sheath to the phloem via the phloem parenchyma (Fig 3.9B). In the phloem, 5,6-CF was localized within the positions predicted for the thin- and thick-walled sieve tubes (Fig 3.9C). These observations suggest that there could be some symplasmic connections along this route and therefore a symplasmic pathway. In transections mounted in silicone oil, where 5,6-CFDA was applied to the transpiration stream, it was cleaved and became fluorescent in the xylem parenchyma. Thereafter an entirely symplasmic pathway was seen at least to the phloem parenchyma.

4.7 Phloem and xylem transport as visualized via 5,6-CF and Texas Red

The data obtained in Fig 3.9A clearly provides evidence for the different functions performed by different bundle orders in sink leaves of *Zea mays* observed after 3h of 5,6-CF transport and 60min of chasing with Texas Red. 5,6-CF was not so evident in the sieve tube of the large vascular bundle and little was moving and diffusing towards the mesophyll cells and therefore providing evidence of transport function by this vein. 'Halo' in the mesophyll of the smaller and intermediate veins supports the view that these veins are involved in the offloading process. Texas Red was always confined within the cells associated with the xylem.

CHAPTER 5: CONCLUSIONS

The potential role of apoplasmic versus symplasmic phloem loading has been revealed for more than 20 years. In *Zea mays*, most of the work has been concerned with ultrastructural and anatomical studies. The central hypothesis on which the thesis rests is based on the assumption that plasmodesmata indicate potential symplasmic pathways. Assimilates are presumed to make use of available symplasmic routes but in *Zea mays,* like many other plants, phloem loading is assumed to be apoplasmic. As such, using a symplasmically-transported fluorochrome such as 5,6-CF should illuminate any functional symplasmic pathway.

Assimilate uptake and transfer is assumed to be via plasmodesmata and therefore 5,6-CF is assumed to be transported via these plasmodesmata. Based on 5,6-CF studies, the maize leaf seems thus to have a symplasmic pathway up to the companion cell-sieve element complex that was not envisaged from previous plasmodesmatal frequency studies. That the thin-walled sieve tubes in the cross veins show 5,6-CF transport and that the fluorochrome was observed within the region of the sieve tube in the retrieval experiments suggest that a symplasmic pathway within the thin-walled sieve tubes possibly follow a path from the BS-MS-VP-CC-ST. Given that the thick-walled sieve tubes are well-connected to the vascular parenchyma (Evert *et al.* 1977) suggests a symplasmic pathway from the BS-MS-VP to the thick-walled sieve tubes.

The slow rate of uptake observed in the maize leaf suggests that the symplasmic loading is not a major route in these species. The data presented here supports a slow symplasmic pathway-perhaps it exists as an alternative to the more efficient apoplasmic process, which makes use of the thin-walled sieve tube in the maize leaf.

Observations from 5,6-CFDA and Texas Red clearly suggest that large bundles are involved mainly in assimilate transport rather than in the loading or unloading processes which were confirmed using source and sink leaf distribution of 5,6-CF.

In source leaves 5,6-CF transport was seen to be basipetal and in sink leaves it was acropetal. Under the experimental conditions *Zea mays* followed the surmized rules governing assimilate transport from source to sink in plants at ambient and elevated CO_2.

Increased rate of uptake of 5,6-CF was observed under elevated CO_2 and at $200\mu m^{-2}sec^{-1}$ light conditions, which suggests an increased capacity for transport and loading of assimilates from the mesophyll to the sieve tubes in the maize leaf. The transport and loading pattern observed in plants undergoing 5,6-CF loading and transport in dark conditions demonstrates that non-photosynthetically-driven phloem transport occurs symplasmically as well.

Although this study was successful in demonstrating a symplasmic route from the mesophyll to the sieve tube-companion cell, further studies need to be done using more appropriate facilities such as Confocal Laser Scanning microscopy (CLSM). Due to limited time constraints and technical problems experienced, little work was carried out using plants exposed to elevated CO_2 and therefore phloem loading and transport studies under elevated CO_2 need to be revisited.

Finally, *Zea mays* appear to have a slow symplasmic phloem loading pathway, and the apoplast can function as a retrieval site for materials that leak into the apoplast including the xylem. However as stated by Farrar *et al.* (1992) the presence of a symplasmic pathway, as demonstrated in this thesis as well, does not necessarily mean that phloem loading is symplasmic under normal conditions.

REFERENCES

Apel P (1976) Grain growth and carbohydrate content in spring wheat at different CO_2-concentrations-Biochem. Physiol. Plflanzen **169**: 355-362

Altus DP, Canny MJ (1982) Loading of assimilates in wheat leaves: I. The specialization of vein types for separate activities. Australian Journal of Plant Physiology **9**: 571-581

Badelt K, White RG, Overall RL, Vesk M (1994) Ultrastructural specialization of the cell wall sleeve around plasmodesmata. American Journal Botany **81**: 1422-1427

Beebe DU, Evert RF (1992) Photoassimilate pathway(s) and phloem loading in the leaf of *Moricandia arvensis* (L) DC (Brassicaceae). Int. J. Plant Sci. **153**: 61-77.

Botha CEJ (1990) Plasmodesmatal structure and frequency in relation to assimilation in C_3 and C_4 grasses in Southern Africa. In: Proceedings of the International Conference on Phloem Transport and Assimilate Compartmentation, Cognac (France), p.9 Bonnemain, J.L., Ed. Univ. de Poitiers, France.

Botha CEJ (1992) Plasmodesmatal distribution, structure and frequency in relation to assimilation inn C_3 and C_4 grasses in Southern Africa. Planta **187**: 348-358

Botha CEJ, Cross RHM (1997) Plasmodesmatal frequency in relation to short distance transport and phloem loading in leaves of Barley (*Hordeum vulgare*). Phloem is not loaded directly from the symplast. Physiologia Plantarum **99**: 355-362

Botha CEJ, Cross RHM (2000) Towards reconciliation of structure with function in plasmodesmata-who is the gatekeeper? Micron **31**: 713-721

Botha CEJ, Cross RHM (2001) Regulation within a supracellular highway-plasmodesma are the key. South African Journal of Botany **67**: 1-9

Botha CEJ, Cross RHM, van Bel AJE, Peter CI (2000) Phloem loading in sucrose-export-defective (SXD-1) mutant maize is limited by callose at plasmodesmata in bundle sheath-vascular parenchyma tissue. Protoplasm **214**: 65-72

Botha CEJ, Evert RF (1986) Free-space marker studies on *Saccharum officinarum* and *Bromus unioloides*. Journal of South African Botany **52**: 335-342.

Botha CEJ, Evert RF (1988) Plasmodesmatal distribution and frequency in vascular bundles and contiguous tissues of the leaf of *Themeda trianda.* Planta **173**: 433-441

Botha CEJ, van Bel AJE (1992) Quantification of symplastic continuity as visualised by plasmodesmograms: diagnostic value for phloem loading pathways. Planta **187**, 359-365

Bourquin S, Bonneman J-L, Delrot S (1990) Inhibition of loading of ^{14}C assimilates by p-chloromercuribenzenesulfonic acid: localization of the apoplastic pathway in *Vicia faba*. Plant Physiology **92**:97-102

Bowes G (1991) Growth at elevated CO_2: photosynthetic responses mediated through Rubisco. Plant Cell Environ **14**: 795-806

Cataldo DA (1974) Vein loading: the role of symplast in intercellular transport of carbohydrates between the mesophyll and the minor vein of tobacco. Plant Physiol **53**: 912-917

Cave G, Tolley LC, Strain BR (1981) Effects of carbon dioxide enrichment on chlorophyll content, starch content and starch grain structure in *Trifolium subterraneum* leaves. Physiologia Plantarum **51**: 171-174

Conroy J, Barlow EWR, Bevege DI (1986) Response of *pinus radiata* seedlings to carbon dioxide enrichment at different levels of water and phosphorus: growth, morphology and anatomy. Annals of Botany **57**: 165-177

Conroy JP, Seneweera S, Bansra AS, Rogers G, Nissen-Wooller B (1994) Influence of rising atmospheric CO_2 concentrations and temperature on growth, yield and grain quality of cereal crops. Australian Journal of Plant Physiology **21**: 741-758

Cure JD, Acock B (1986) Crop responses to carbon dioxide doubling: A literature survey. Agricultural and Forest Metereology **38**: 127-145

Currier HB (1957) Callose substance in plant cells. American Journal of Botany **44**: 478-488

Currier HB, Strugger S (1955) Aniline blue and fluorescence microscopy of callose in bulb scales of *Allium cepa* L

Delrot S (1989) Loading of photoassimilates. In Barker DA, Milburn JA (eds) Transport of photoassimilates. John Wiley & Sons Inc., New York, pp 167-205

Ding B, Parthasarathy MV, Niklas K, Turgeon R (1988) A morphometric analysis of the phloem-unloading pathway in developing tobacco leaves. Planta **176**: 307-318

Ding B, Haudenshield JS, Hull RJ, Wolf S, Beachy RN, Lucas WJ (1992) Secondary plasmodesmata are specific sites of localization of the tobacco mosaic movement protein in transgenic tobacco plants. Plant cell **4**: 915-928

Epel BL (1994) Plasmodesmata: composition, structure and trafficking. Plant Mol. Bio. **26**: 1343-1356

Erwee MG, Goodwin PB (1983) Charactrisation of the *Egeria densa* Planch. leaf symplast: inhibition of the intercellular movement of fluorescent probes by group 2 ions. Planta **158**: 320-328

Erwee MG, Goodwin PB, van Bel AJE (1985) Cell-cell communication in the leaves of *Commelina cyanea* and other plants. Plant Cell Environ **8**:173-178

Esau K (1977) Anatomy of seed plants 2nd edn. Wiley, New York Santa Barbara London Sydney Toronto pp 67-81

Evert RF (1980) Vascular anatomy of angiosperm leaves with special consideration of the maize leaf. Ber. Dtsch. Bot. Ges. **93**: 43-45

Evert RF (1986) Phloem loading in maize. In: Regulation of carbon and nitrogen reduction and utilization in maize JC Shannpn DP Knievel and CD Bayer eds. American Society of Plant Physiologists 67-81

Evert RF, Botha CEJ, Mierzwa RJ (1985) Free space marker studies on the leaf of *Zea mays* L. Protoplasma **126**: 62-73

Evert RF, Eschrich W, Heyser W (1978) Leaf structure in relation to solute transport and phloem loading in *Zea mays* L. Planta **138**: 279-294

Evert RF, Eschrich W, Heyser W (1977a) Distribution and structure of the plasmodesmata in mesophyll and bundle-sheath cells of Zea mays. Planta **136**: 77-89

Evert RF, Eschrich W, Neuberg DS, Eichhorn SE (1977b) Tubular extensions of plasmalemma in leaf cell of *Zea mays* L. Planta **135**: 203-205

Evert RF, Mierzwa RJ (1986) Pathway(s) of assimilate movement from mesophyll cells to sieve tubes in the *Beta vulgaris* leaf. In: Phloem transport, pp 419-432. Cronshaw, J; Lucas WJ, Giaquinta RT, eds. Alan R. Liss, Inc., New York

Evert RF, Mierzwa RJ (1989) The cell wall plasmalemma interface in sieve tubes in Barley. Planta **177**: 24-34

Evert RF and Russin W (1993). Structurally phloem unloading in the maize leaf cannot be symplastic. American Journal of Botany **80**: 1310-1317.

Evert RF, Russin WA, Botha CEJ (1996) Distribution and frequency of plasmodesmata in relation to photoassimilate pathways and phloem loading in Barley leaf. Planta **198**: 572-579.

Farrar J, van der Schoot C, Drent P, van Bel AJE (1992) Symplasmic transport of Lucifer yellow in mature leaf blades of barley: Potential mesophyll-to-sieve-tube transfer. New Phytol **120**:191-196

Fisher DG (1986) Ultrastructure, plasmodesmatal frequency, and solute concentration in green area of variegated *Coleus blumei Benth* leaves. Planta **169**: 141-152

Fisher DG (1988) Movement of Lucifer Yellow in leaves of *Coleus blumei* Benth. Plant Cell and Environ **11**: 639-644

Fisher DG, Evert RF (1982) Studies in the leaf of *Amaranthus retroflexus* (*Amaranthaceae*): Ultrastructure, plasmodesmatal frequency and solute concentration in relation to phloem loading. Planta **155**: 377-387

Flora LL, Madore MA (1996) Significance of minor-vein anatomy to carbohydrate transport. Planta **198**: 171-178

Fritz E, Evert RF, Nasse H (1989) Loading and transport of assimilates in different maize leaf bundles. Digital image analysis of ^{14}C microautoradiographs. Planta **178**: 1-9

Fritz E, Evert RF, Weyser W (1983) Microautoradiographic studies of phloem loading and transport in the leaf of *Zea mays* L. Planta **159**: 193-206

Gamalei YV (1996) Membrane compartmentation and cell-to-cell transport of photosynthates. Journal of Experimental Botany **47**: 1297

Gamalei YV, Pakhomova MV (1981) Distribution of plasmodesmata and parenchyma transport of assimilates in leaves of several dicots. Sov. Plant Physiol **28**: 649-661

Gamalei YV, Pakhomova MV, Sjntkina AV (1994). Regulation of assimilate translocation by plasmodesmata: effect of temperature and water stress. In: Workshop on Basic and Applied Research in Plasmodesmatal Biology (Israel) pp 132-135

Geiger DR (1975) Phloem loading. In Zimmermann, JA Milbourne eds. Transport in plants 1. Springer-verlag, Heidelberg, pp 395-450

Giaquinta RF (1989) Phloem loading of sucrose. Plant Physiology **63**: 744-748

Giaquinta RT (1980) Translocation of sucrose and oligosaccharides. In: The biochemistry of plants, vol 3, pp. 271-320, Preiss, J., ed. Academic Press, New York London Sydney

Giaquinta RT (1983) Phloem loading of sucrose. Annu. Rev. Plant Physiol. **34**: 347-387

Goodwin B P (1983) Molecular size limit for movement in the symplast of the *Elodea* leaf. Planta **157**: 124-130

Grignon N, Tourain B, Durand M (1989) 6(5) carboxyfluorescein as a tracer of phloem sap translocation. American Journal of Botany **76**: 871-877

Gunning BES (1976) The role of plasmodesmata is short distance transport to and from the phloem. In MH Zimmermann, JA Milbourn eds. Transport in plants 1. Springer-verlag, Heidelberg,pp203-227

Hartt CE (1966) Translocation in colored light. Plant Physiology **41**: 369-372

Haupt S, Duncan GH, Holzberg S, Oparka KJ (2001) Evidence of symplasmic phloem unloading in sink leaves of Barley. Plant Physiology **125**: 209-218

Heineke D, Kauder F, Frommer W, Kumn C, Gillissen B, Ludewig F, Sonnewald U (1999) Application of transgenic plants in understanding responses to atmospheric change. Plant Cell Environ **22**: 623-628

Hewitt EJ (1966) Sand and water culture methods used in the study of plant nutrition. Tech. Commun 22 (revised), Commonwealth Bureau of Horticultural and Plantation Crops, East Mall ing. Commonwealth Agric. Bireau, Farnham Royal, England. (See appendix)

Heyser W, Leonard O, Heyser R, Fritz E, Eschrich W (1975) The influence of light, darkness and lack of CO_2 on phloem translocation in detached maize leaves. Planta **122**: 143-154

Ho LC (1977) Effects of CO_2 enrichment on the rates of photosynthesis and translocation of tomato leaves. Annals of Applied Biology **87**: 191-200

Hughes JE, Gunning BES (1980) Glutaraldehyde-induced deposition of callose. Canadian Journal of Botany **58**: 250-258

Kalt-Torres W, Kerr PS, Usuda H, Huber SC (1987) Diurnal changes in maize leaf photosynthesis. Plant Physiology **83**: 283-288

Kleier DA (1988) Phloem mobility of Xenobiotics. I Mathematical model unifying the weak acid and intermediate permeability theories. Plant Physiology **86**: 803-810

Komor E (2000) Source physiology and assimilate transport: the interaction of transport metabolism, starch storage and phloem export in source leaves and the effects on sugar status in phloem. Australian Journal of Plant Physiology **27**:497-505

Korner CH, Palaez-Riedl S, van Bel AJE (1995) CO_2 responsiveness of plants: a possible link to phloem loading. Plant Cell and Environment **18**: 595-600

Kutik J, Natr L, Demmers-Derks HH, Lawlor DW (1995) Chloroplast ultrastructure of sugar beet (Beta vulgaris L.) cultivated in normal and elevated CO_2 concentration with two nitrogen supplies. Journal of Experimental Botany **46**: 1797-1802

Kuo J, O'Brien TP (1974) Lignified sieve elements in wheat leaf. Planta **117**: 349-353

Läuchli A (1976) Apoplastic transport in tissues. In: Transport in plants, pp 3-34, Lüttge, U., Pitman, M.G., eds. Berlin-Heidel-berg-New York: Springer 1976

Lawler DH, Mitchell RAC (1991) The effects of increasing CO_2 on crop photosynthesis and productivity: a review of field studies. Plant Cell Environ **14**: 807-818

Lee DR (1981) Elasticity of phloem tissues. Journal of Experimental botany **32**: 251-260

Lucas WJ, Ding B, Van Der Schoot C (1993) Transley Review no. 58 Plasmodesmata and the supracellular nature of plants. New Phytol **125**: 435-476

Lush WM (1976) Leaf structure and translocation of dry matter in C_3 and C_4 grasses. Planta **130**: 235-244

Madore MA, Lucas WJ (1987) Control of photoassimilate movement in source leaf tissue of *Ipomoea tricolor* Cav. Planta **171**: 197-204

Madore MA, Oross JW, Lucas WJ (1986) Symplastic transportation in *Ipomea tricolor* source leaves. Demonstration of functional symplasmic connections from mesophyll to minor vein by a novel dye-tracer method. Plant Physiology **82**: 432-442

Madore MA, Webb JA (1981) Leaf free space analysis and vein loading in *Curcubita pepo*. Canadian Journal of Botany **59**: 2550-2557

Madsen E (1968) Effects of CO_2 concentration on the accumulation of starch and sugar in tomatoe leaves. Physiologia Plantarum **21**: 168-185

Matsiliza B, Botha CEJ (2002) Aphid *Stobion yakini* investigation suggests that thin-walled sieve tubes in Barley (*Hordeum vulgare* L.) to be more functional than thick-walled sieve tubes. Physiologia Plantarum **115**: 137-143

McLean BG, Hempel FD, Zambryski PC (1997) Plant intercellular communication via plasmodesmata. Plant Cell **9**: 1043-1054

Miller DKE, Griffiths E, Lennard J, Firestone RA (1983) Cell killing by lysosomotropic detergents. Journal of Cell Biology **97**: 1841-1851

Nafziger ED, Koller RH (1976) Influence of leaf starch concentration on CO_2 assimilation in soybeans. Plant physiology **57**: 560-563

Oparka KJ (1991) Uptake and compartmentation of fluorescent Probes by plant cells. Journal of Experimental Botany **42**: 565-579

Oparka KJ, Duckett CM, Prior DAM, Fisher DB (1994) Real time imaging of phloem unloading in the root tip of *Arabidopsis*. Plant Journal **6**: 759-766

Oparka K, Turgeon R (1999) Sieve elements and companion cells-traffic control centres of the phloem. The Plant Cell **11**: 739-750

Oparka KJ, Van Bel AJE (1992) Pathways of phloem loading and unloading: a plea for uniform terminology. In: Carbon Partitioning Within and Between Organisms (Farrar JF, Gordon AJ, Pollock CJ eds) Bios Oxford, pp 249-254

Preiss J (1982) Regulation of the biosynthesis and degradation of starch. Ann. Rev. Plant Physiol. **33**: 431-454

Pritchard SG, Peterson CM, Reunion GB, Prior SA, Rogers HH (1997) Atmospheric CO_2 concentration, N availability, and water status effect pattern of ergastic substance deposition in longleaf pine (*Pinus palustris Mill.*) foliage. Trees, in press

Radford JE, Vesk M, Overall RL (1998) Callose deposition at plasmodesmata. Protoplasma **201**: 30-37

Robards AW, Lucas WJ (1990) Plasmodesmata. Annual Review of Plant Physiology Plant Molecular Biology **41**: 369-419

Roberts AG, Santa Cruz S, Roberts IM, Prior DAM, Turgeon R (1997) Phloem unloading in sink leaves of *Nicotiana benthamiana*: comparison of a fluorescent solute with a fluorescent virus. Plant Cell **9**: 1381-1396

Robinson-Beers K, Evert RF (1991) Ultrastructure of and plasmodesmatal frequency in mature leaves of sugarcane. Planta **184**: 291-306.

Russell SH, Evert RF (1985) Leaf vasculature in *Zea mays* L. Planta **164**:448-458

Russin WA, Evert RF (1985) Studies on the leaf of *Populus deltoides* (Salicaceae): Ultrastructure, plasmodesmatal frequency and solute concentrations. American Journal of Botany: **72**: 1232-1247

Russin WA, Evert RF, Vanderveer PJ, Sharkey TD, Briggs SP (1996) Modification of a specific class of plasmodesmata and loss of sucrose export ability in the sucrose export defective 1 maize mutant. Plant Cell **8**: 645-658

Schmitz K, Cuypers B, Moll M (1987) Pathways and assimilate transfer between mesophyll cells and minor veins in leaves of *Cucumus melo*. Planta **171**:19-29

Schulze A (1999) Physiological control of plasmodesmal gating. In: van Bel AJE, van Kesteren WJP (eds) Plasmodesmata: structure, function, role in cell communication. Springer, Berlin Heidelberg New York Tokyo, pp 173-204

Smith MM, McCully ME (1978) A critical evaluation of the specifity of aniline blue induced fluorescence. Protoplasma **95**: 229-254

Stewart WW (1981) Lucifer dyes-highly fluorescent dyes for biological tracing. Nature **292**: 17-21

Stitt M (1991) Rising CO_2 levels and their potential significance for carbon flow in photosynthetic cells. Plant Cell Environ **14**: 741-762

St Omer L, Horvath SM (1984) Developmental changes in anatomy, morphology and biochemistry of *Layia platyglossa* exposed to elevated carbon dioxide. American Journal of Botany **71**: 693-699

Terry BR, Robards AW (1987) Hydrodynamic radius alone governs the mobility of molecules through plasmodesmata. Planta **171**:145-157

Thomas JF, Harvey CH (1983) Leaf anatomy of four species grown under continuous CO_2 enrichment. Botanical Gazzete **144**: 303-309

Turgeon R (1987) Phloem unloading in tobacco sink leaves: insensitivity to anoxia indicates a symplastic pathway. Planta **171**: 73-81

Turgeon R (1989) The sink-source transition in leaves. Annual Review of Plant Physiology and Plant Molecular Biology **40**: 119-138

Turgeon R (2000) Plasmodesmata and solute exchange in the phloem. Australian Journal of Plant Physiology **27**: 521-529

Turgeon R, Beebe DU (1991). The evidence for symplastic phloem loading. Plant Physiology **196**: 349-354

Turgeon R, Beebe DU, Gowan E (1993) The intermediary cell: Minor-vein anatomy and raffinose oligosaccharide synthesis in the *Scrophulariaceae*. Planta **191**: 446-456

Turgeon R, Gowan E (1990) Phloem loading in *Coleus blumei* in the absence of carrier mediated uptake of export sugars from the apoplast. Plant Physiology **94**: 1244-1249

Turgeon R, Hepler PK (1989) Symplastic continuity between mesophyll and companion cells in minor veins of mature *Cucurbita pepo* L. leaves. Planta **179**:24-31

Turgeon R, Webb JA, Evert RF (1975) Ultrastructure of minor veins in *Cucurbita pepo* leaves. Protoplasma **83**: 217-232

Turgeon R, Wimmers L (1988) Different parttens of vein loading of exogenous (^{14}C)-sucrose in leaves of *Psium sativum* and *Coleus blumei*. Plant Physiology **87**: 179-182

Turker EB, Boss WF (1996) Mastoparan-induced intracellular Ca^{2+} fluxes may regulate cell-to-cell communication in plants. Plant Physiology **111**: 459-467

Turker JE, Mauzerall D, Turker EB (1989) Symplastic transport of carboxyfluorescein in staminal hairs of *Setcreasea purpurea* is diffusive and includes loss to the vacuole. Plant Physiology **90**: 1143-1147

van Bel AJE (1996) Carbohydrate processing in the mesophyll trajectry in symplasmic and apoplasmic phloem loading. Progress in Botany **56**: 140-167

van Bel AJE, Knoblauch M (2000) Sieve element and companion cell: the story of the comatose patient and the hyperactive nurse. Australian Journal of Plant Physiology **27**: 477-489.

van Bel AJE, Gamalei Y, Ammerlaan A, Bik LPM (1992) Dissimilar phloem loading in leaves with symplastic and apoplastic minor vein configurations. Planta **186**: 518-525

van Bel AJE, Koops AJ (1985) Uptake of ^{14}C-sucrose in isolated minor vein networks of *Commelina benghalensis* L. Planta **164**: 362-369

van Bel AJE, Oparka KJ (1995) On the validity of plasmodesmograms. Bot. Acta **108**: 174-182

van Bel AJE, Van Kesteren WJP, Papenhuijzen C (1988) Ultrastructural indications for coexistence of symplastic and apoplastic phloem loading in *Commelina benghalensis* leaves: differences in ontogenic development, spatial arrangement and symplastic connections of the two sieve tubes in the minor vein. Planta **176**: 159-172

Van der Schoot C, Rinne P (1999) The symplasmic organization of the shoot apical meristem. In: van Bel AJE, van Kesteren WJP (eds) Plasmodesmata Structure, Function, Role in cell communication. Springer-verlag, Berlin, pp 226-242

Van Kesteren WJP,Van der Schoot C, van Bel AJE (1988) Symplastic transfer of fluorescent dyes from mesophyll to sieve tube in stripped leaf tissue and partly isolated minor veins of *Commelina benghalensis*. Plant Physiology **88**:667-670

Vu JC, Allen LH, Bowes G (1989) Leaf ultrastructure, carbohydrates and protein of soybeans grown under CO_2 enrichment. Environmental and Experimental Botany **29**: 141-147

Walsh MA (1974) Late-formed metaphloem sieve-elements in *Zea mays*. Planta **121**: 17-25

Warmbrodt RD, Van Der Woude WJ (1990) Leaf of *Spinacia oleracea* (spinach): ultrastructure and plasmodesmatal distribution and frequency in relation to sieve-tube loading. American Journal of Botany 77: 1361-1377

Weisberg LA, Wimmers LE, Turgeon R (1988) Photoassimilate transport characteristics of nonchlorophyllous and green tissue in variegated leaves of *Coleus blumei*. Planta **175**: 1-8

Willie AC, Lucas WJ (1984) Ultrastructural and histochemical studies in guard cells. Planta **160**: 129-142

White RG, Badelt K, Overall RL, Vesk M (1994) Actin associated with plasmodesmata. Protoplasma **180**: 169-184

Wolfe DW, Erickson JD (1993) Carbon dioxide effects on plants: Uncertainties and implications for modeling crop response to climate change. In: Agricultural Dimensions of Global Climate Change. (Kaiser HM, Drennen TE eds.) pp 153-178 St. Lucie Press, Delray Beach, Florida

Woodrow IE (1994) Optimal acclimation of C_3 photosynthetic systems under enhanced CO_2. Photosynthesis research **39**: 401-402

Wright KM, Oparka KJ (1996) The fluorescent probe HPTS as a phloem-mobile, symplastic tracer: an evaluation using confocal laser scanning microscopy. Journal of Experimental Botany **47**: 439-445

APPENDIX A

The full Long-Ashton nutrient solution used in this study as taken from Hewitt (1966).

	Wt used (g)	**V. stock Sol. (ml)**	**V. stock sol. dil. In 25 L (ml)**	**Conc. In final V. of 25 L (mM0**
Macronutrient				
KNO_3	101	500	25	2
K_2SO_4	43	500	25	1
$Ca(NO_3)_2$	164	500	25	4
$CaCl_2$	111	500	25	4
$MgSO_47H_20$	92	500	25	1.5
$NaH_2PO_4.2H_2O$	104	500	25	4
Micronutrient				
$MnSO_4.4H_2O$	11.20	500	2.5	0.02
$CuSO_4.5H_2O$	1.25	500	2.5	0.002
$ZnSO_4.7H_2O$	1.45	500	2.5	0.002
H_3BO_3	15.50	500	2.5	0.05
$Na_2Mo_4.2H_2O$	0.605	500	2.5	0.0005
NaCl	29.30	500	2.5	0.1
Fe-Citrate (3H2O)	29.90	500	2.5	0.6

APPENDIX B

Table 1: Alcohol dehydration series (from Botha, 1994)

	Step	Time in hours
1.	FAA	24h
2.	50% EtOH	12h
3.	70% EtOH	12h
4.	35% Butyl-alcohol	12h
5.	55% Butyl-alcohol	12h
6.	75% Butyl-alcohol	12h
7.	100% Butyl-alcohol	3 changes of 12 hours each
8.	100% n-Butanol (liquid parrafin)	12h

Table 2: Composition of F.A.A.

Ethyl alcohol	50 cc
Glacial acetic acid	5 cc
Formaldehyde (37-40 %)	10 cc
Water	35 cc

Table 3.: Staining series (from Botha, 1994)

	Stain	Time
1.	Xylol	3 min
2.	Xylol	3 min
3.	Xylol	3 min
4.	Xylol : Alc. 50 : 50	3 min
5.	Abs. Alc.	2 min
6.	90% Alc.	2 min
7.	70% Alc.	2 min
8.	50% Alc.	2 min
9.	Safranin	24 hours
10.	70% Alc.	2 min
11.	90% Alc.	2 min
12.	95% Alc. + picric acid	dip drain
13.	95% Alc.= NH_3	dip drain
14.	Abs. Alc.	2 min
15.	Abs. Alc.	2 min
16.	Fast green	1 min
17.	clove oil	dip drain
18.	clearer	dip drain
19.	Xylol	2 min
20.	Xylol	2 min
21.	Xylol	max. 5-6 min